Figure 4.1

a. System showing input and output;
b. pole-zero plot of the system;
c. evolution of a system response. Follow blue arrows to see the evolution of the response component generated by the pole or zero.

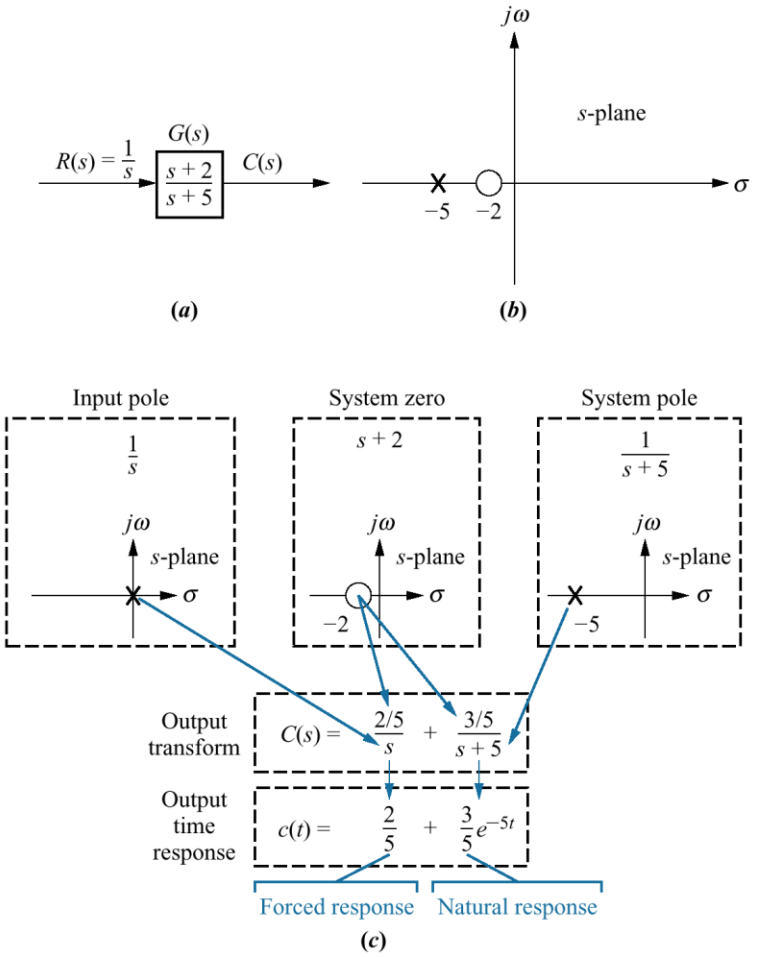

Figure 4.2
Effect of a real-axis pole upon transient response

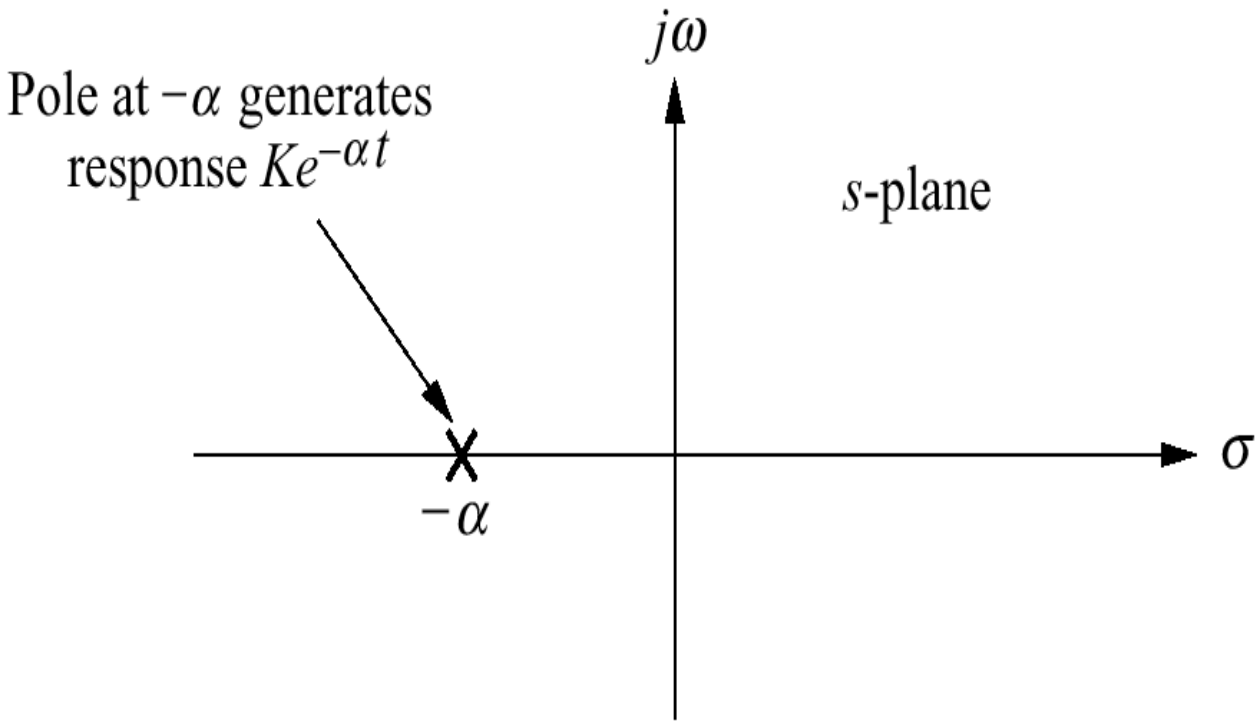

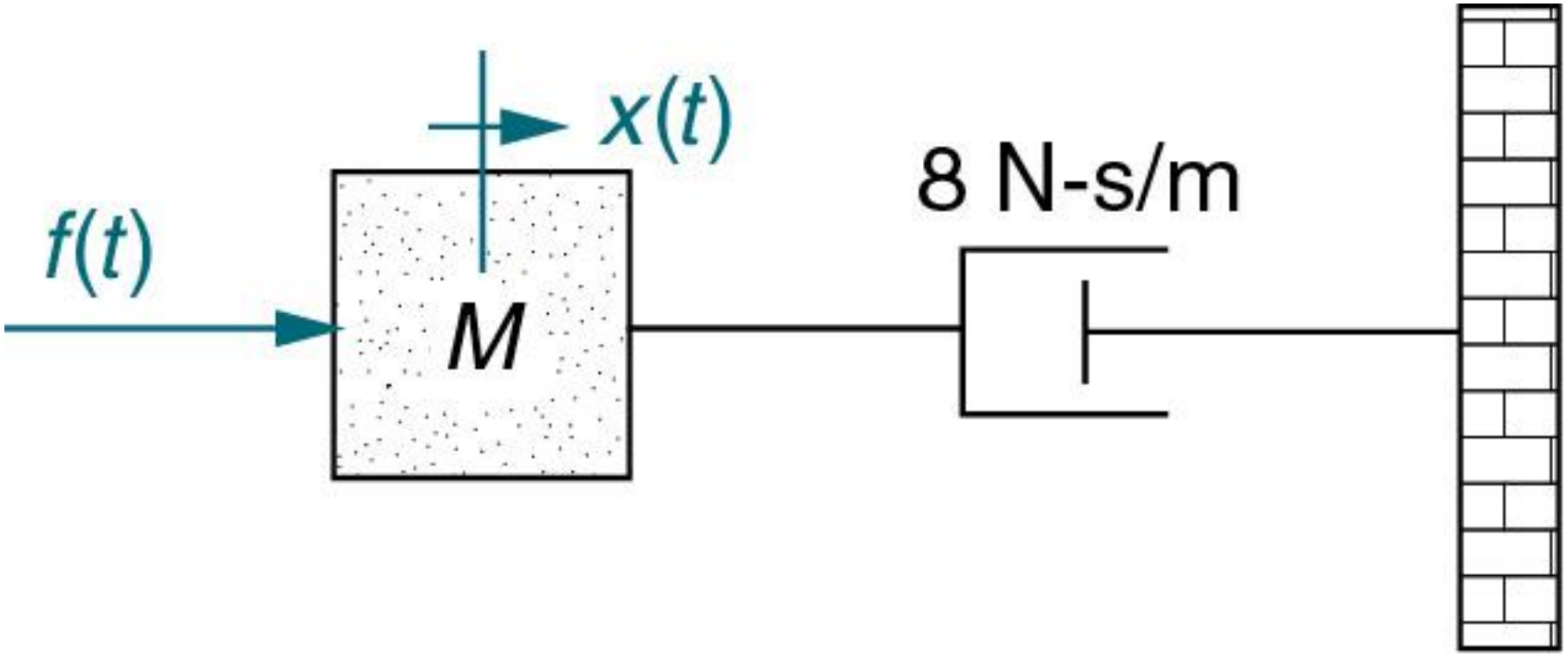

Figure 4-3 (p. 234)

Figure 4.4
a. First-order system;
b. pole plot

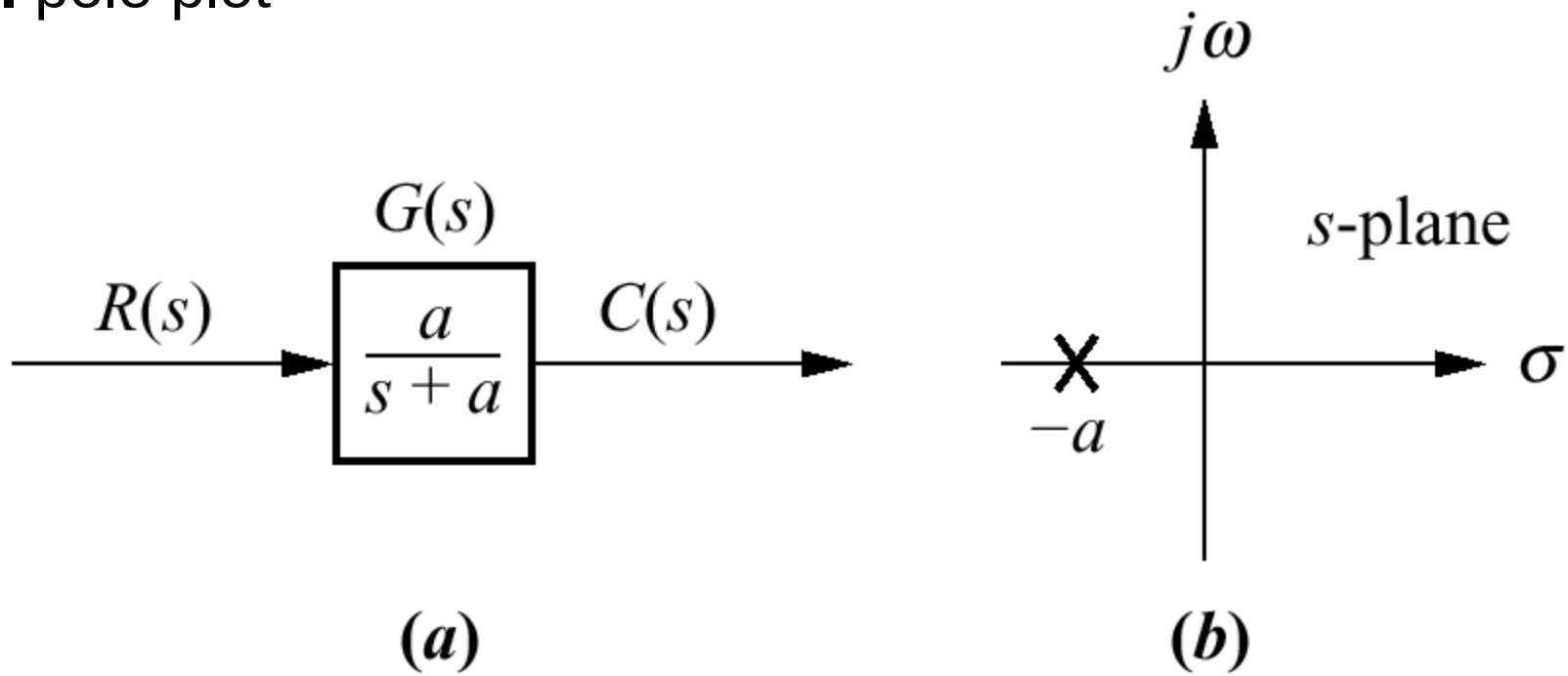

Figure 4.5
First-order system response to a unit step

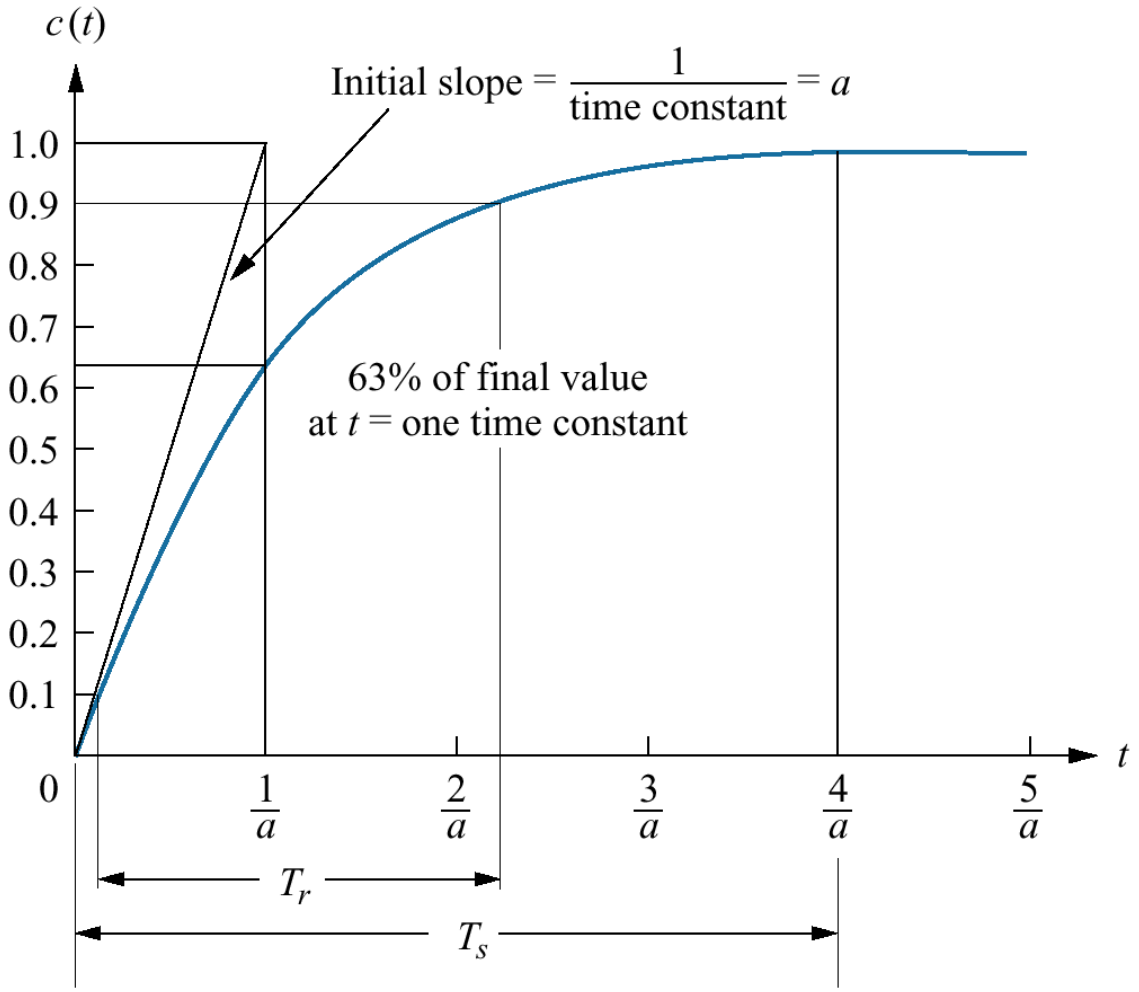

Figure 4.6
Laboratory results of a system step response test

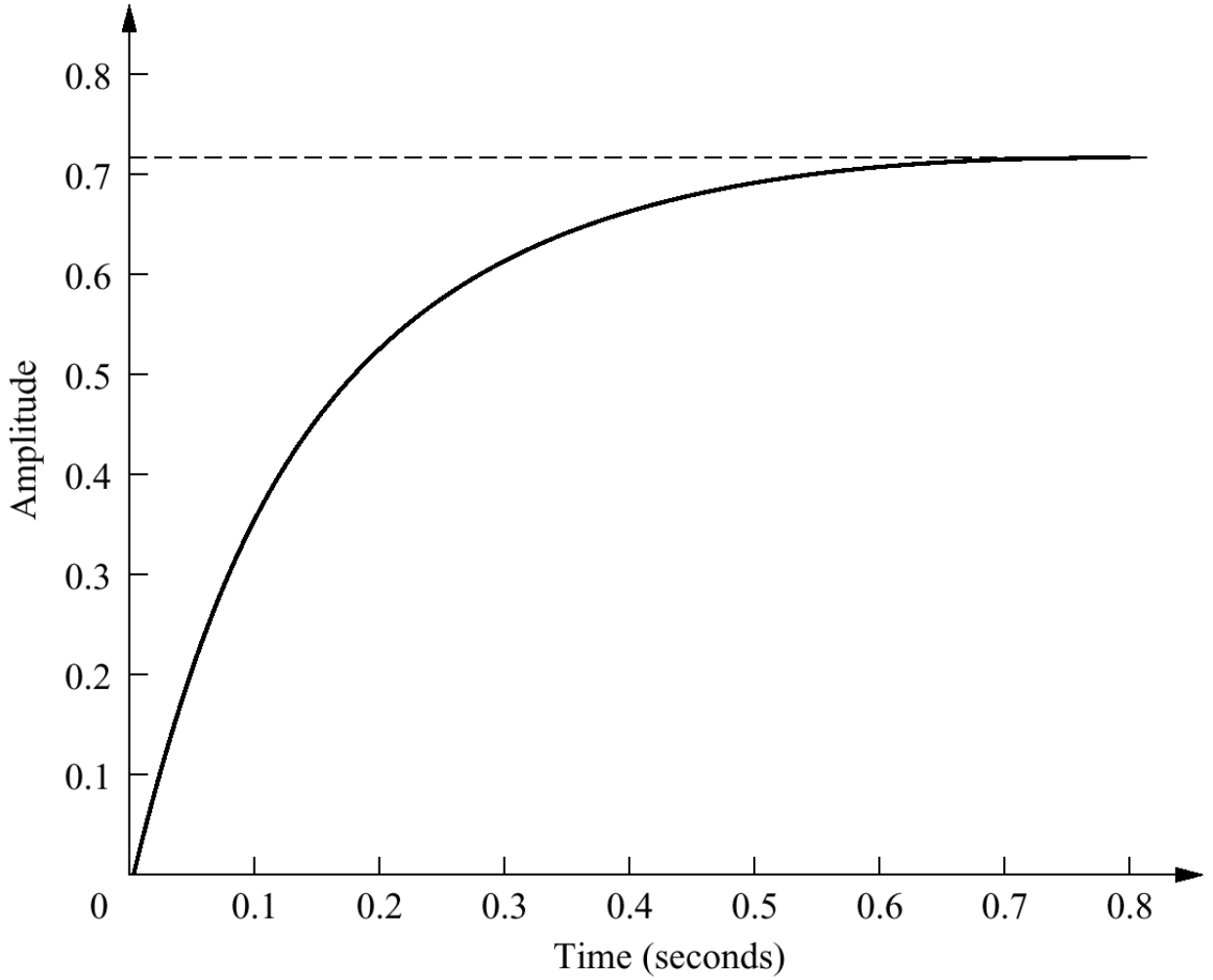

Figure 4.7
Second-order systems, pole plots, and step responses

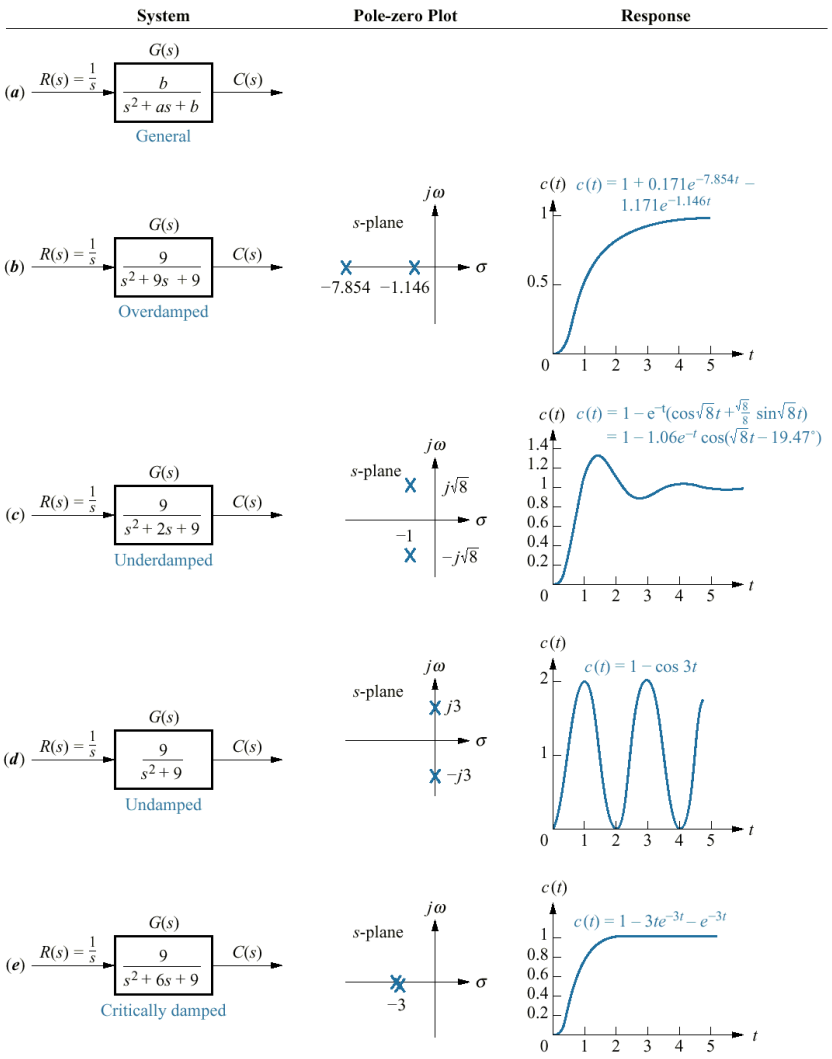

Figure 4.8
Second-order step response components generated by complex poles

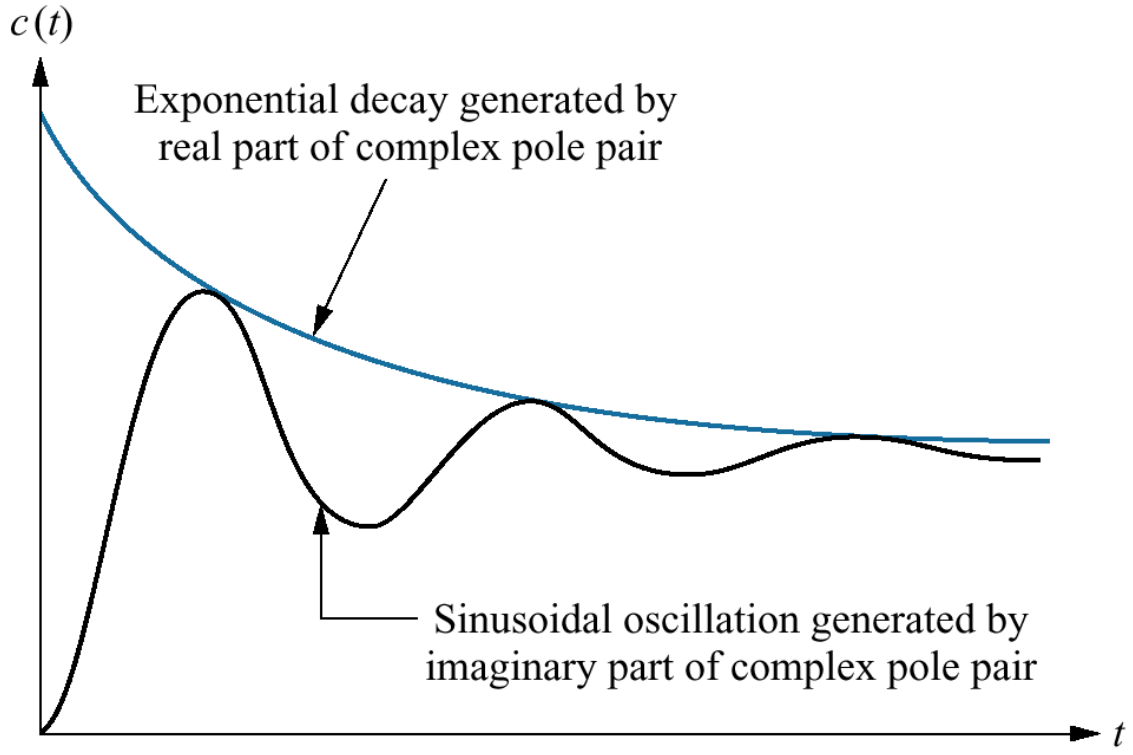

Figure 4.9
System for
Example 4.2

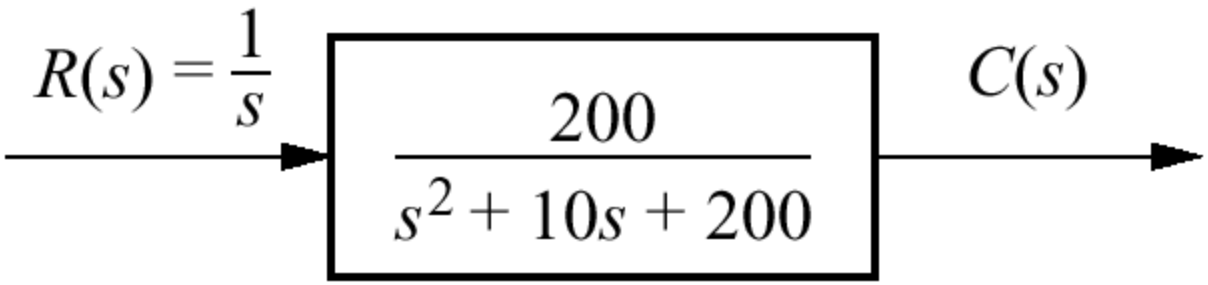

Figure 4.10
Step responses for second-order system damping cases

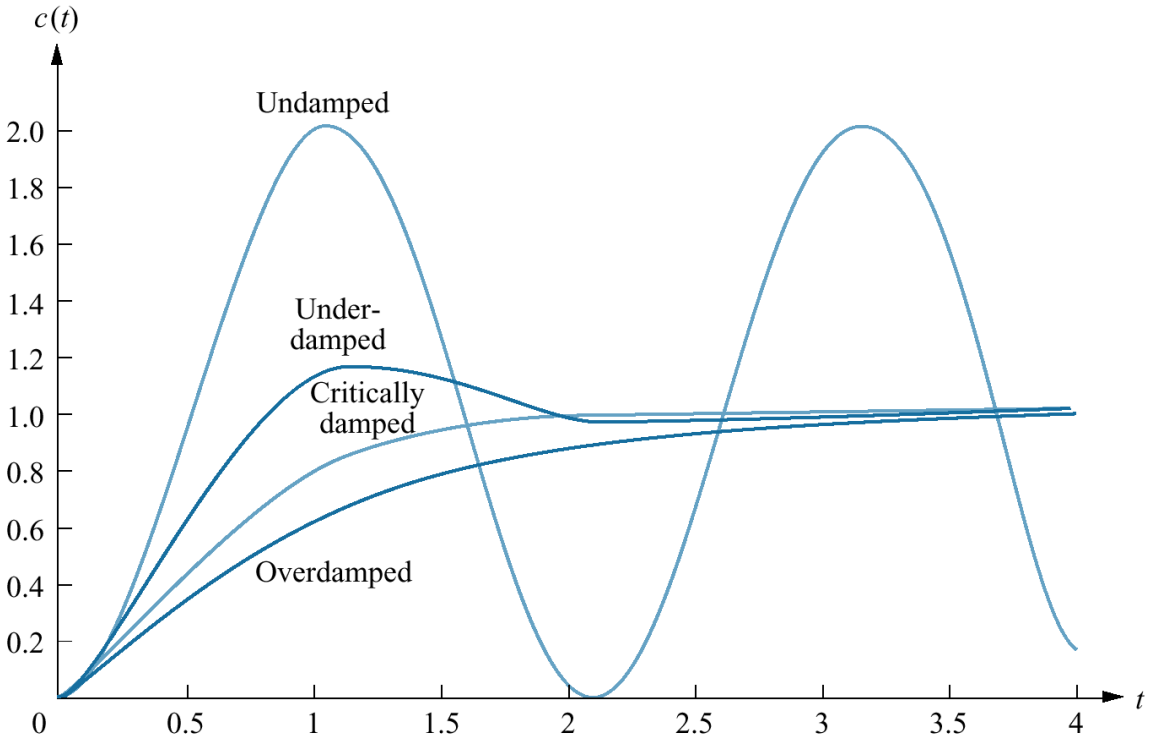

Figure 4.11
Second-order response as a function of damping ratio

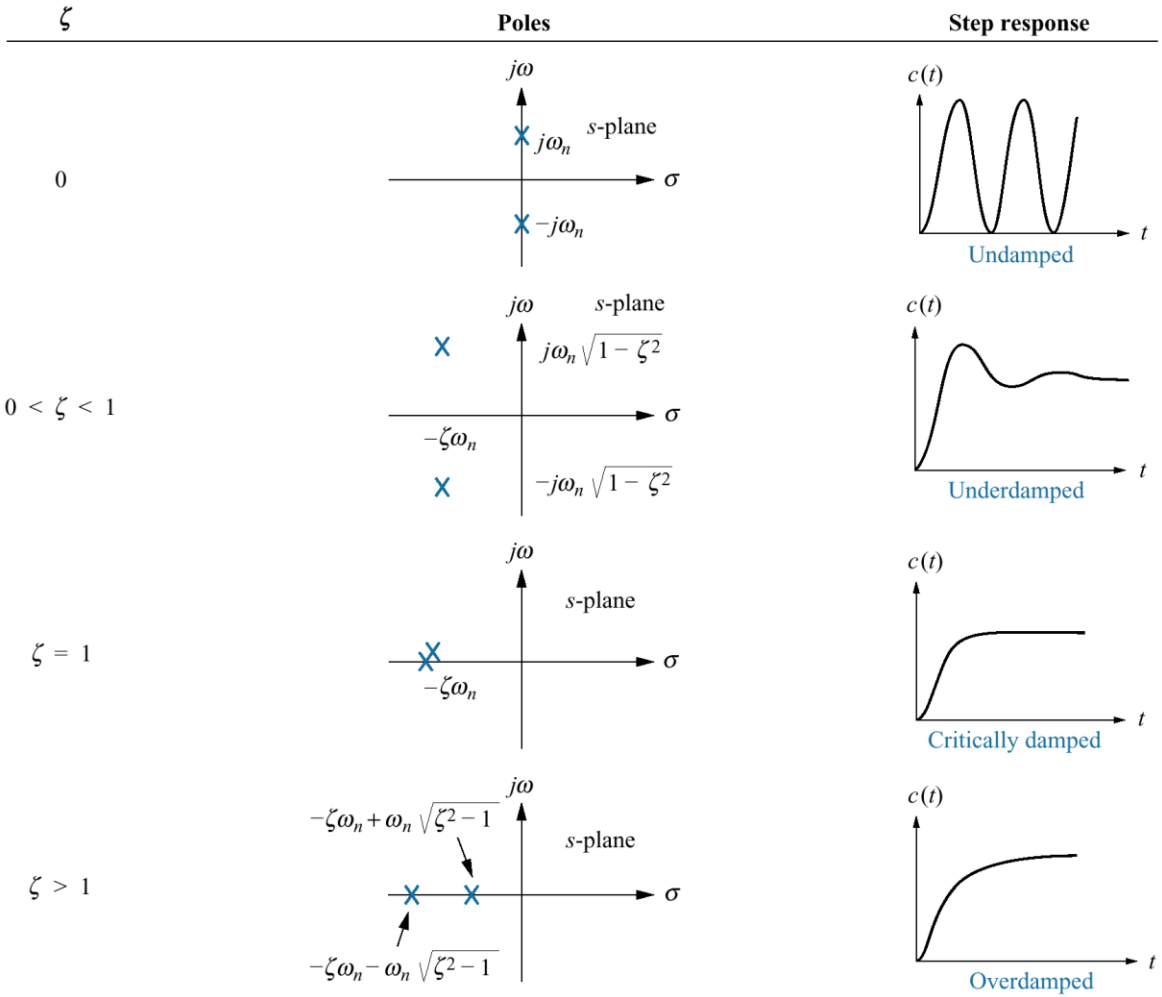

Figure 4.12
Systems for
Example 4.4

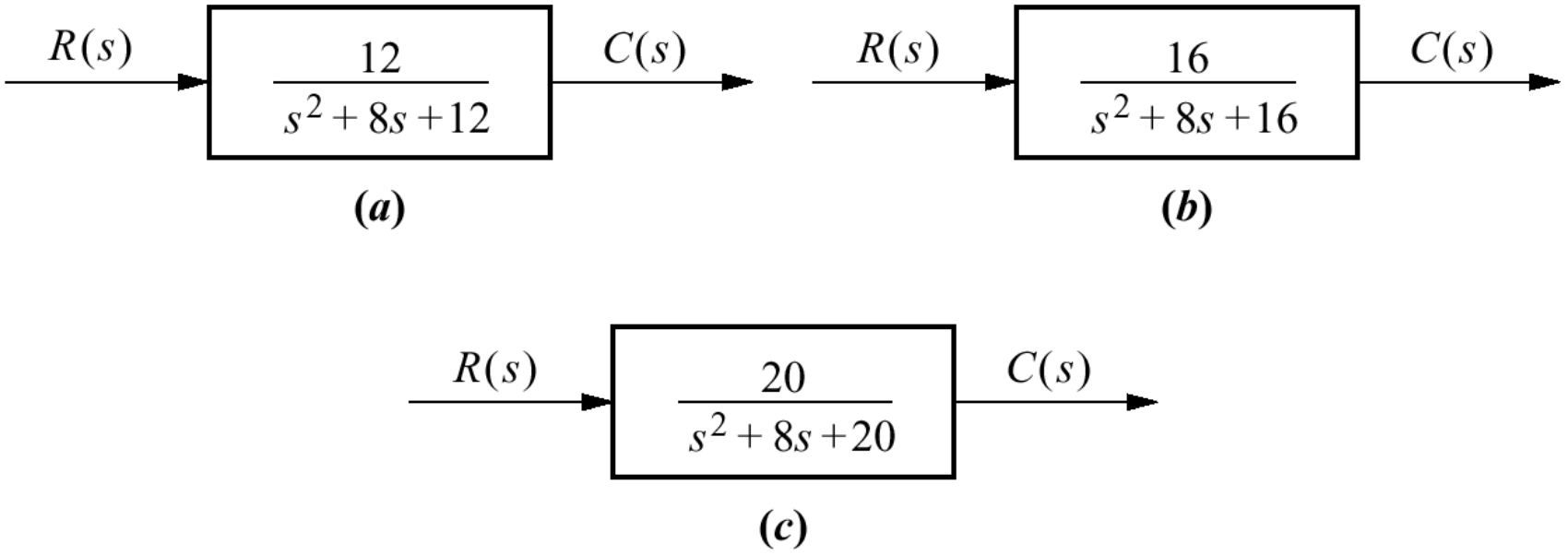

Figure 4.13
Second-order underdamped responses for damping ratio values

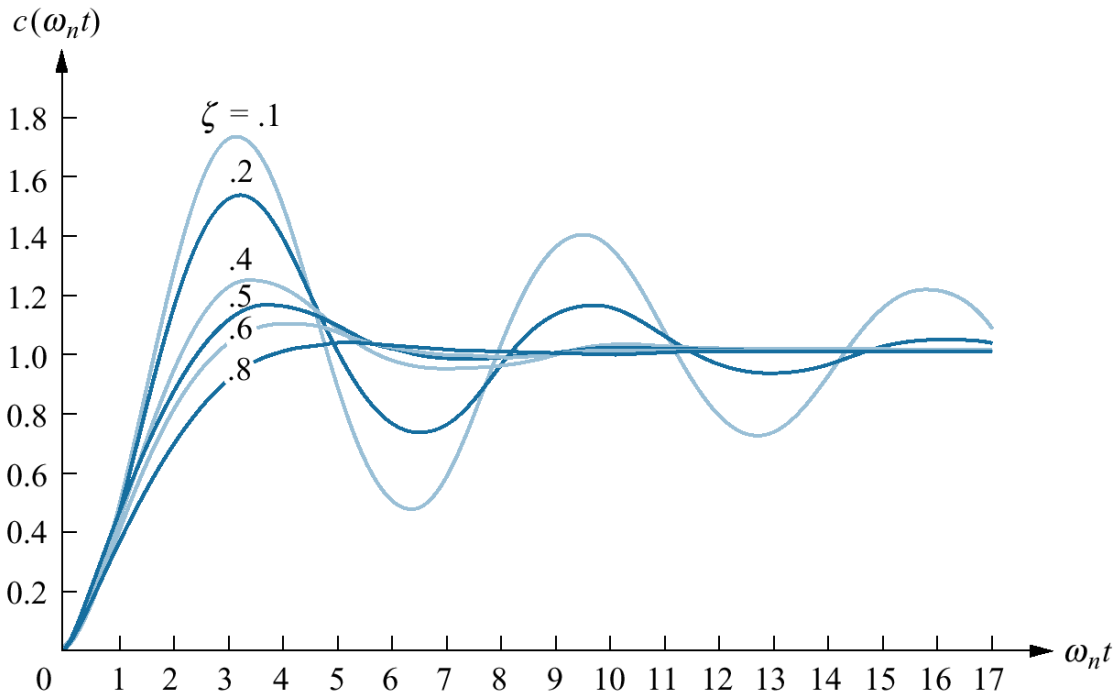

Figure 4.14
Second-order underdamped response specifications

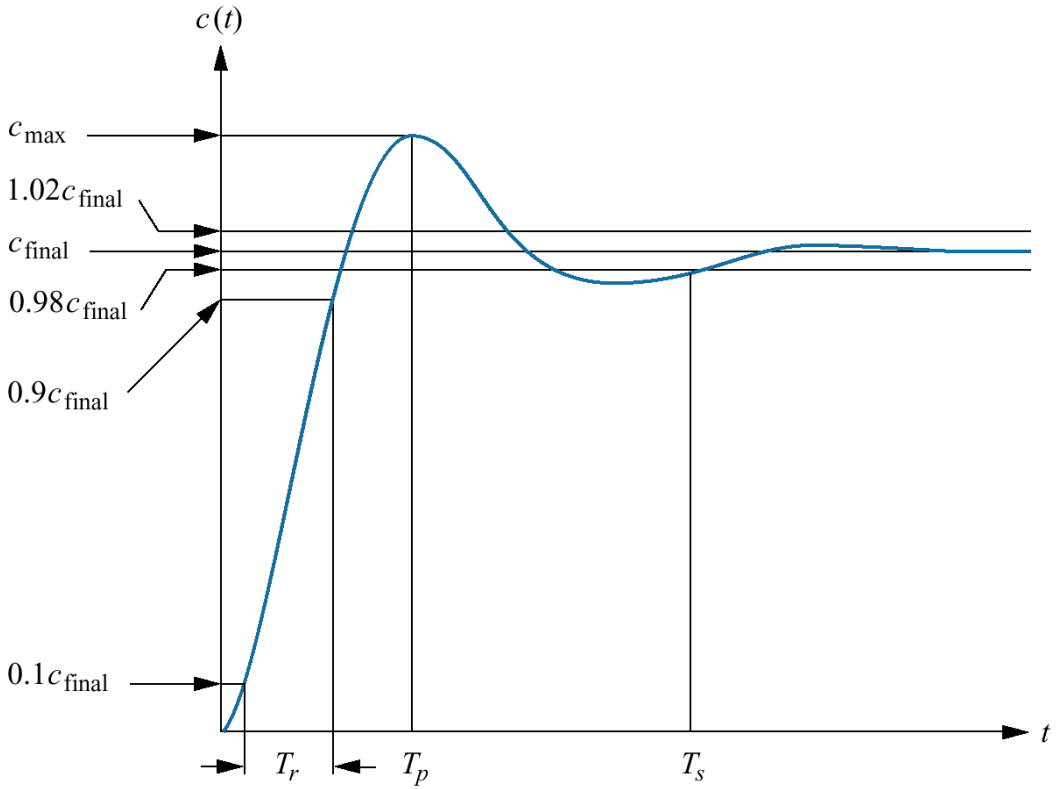

Figure 4.15
Percent overshoot vs. damping ratio

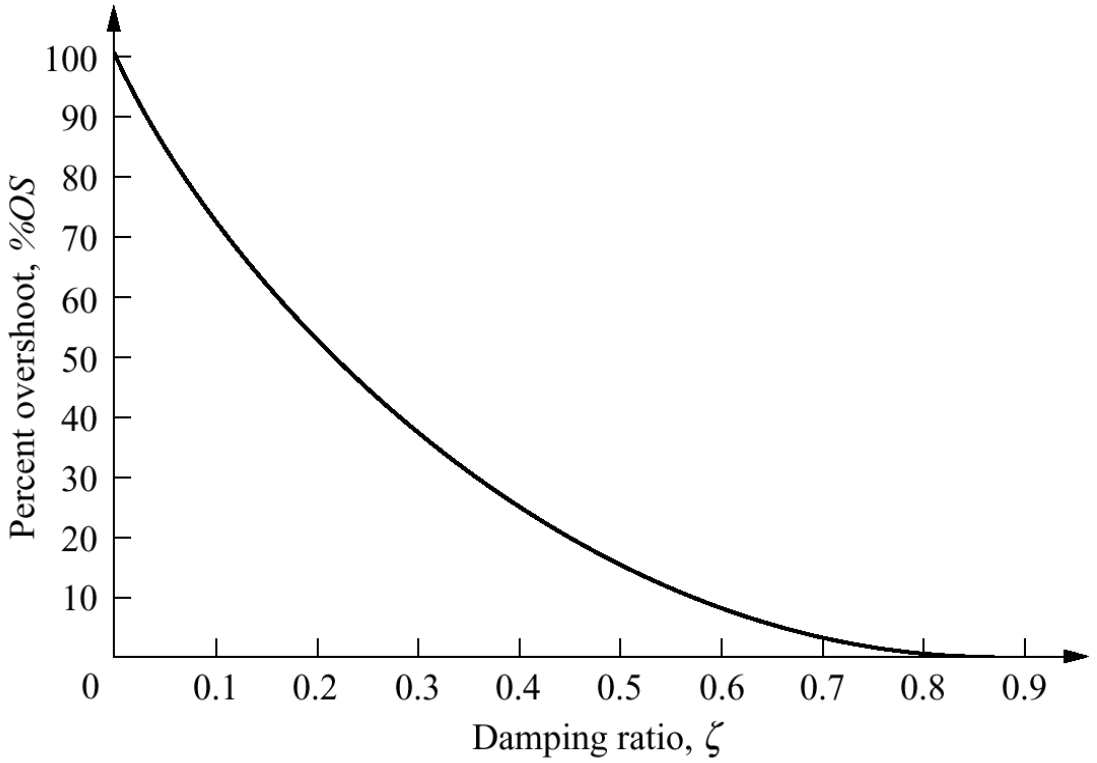

Figure 4.16
Normalized rise time vs. damping ratio for a second-order underdamped response

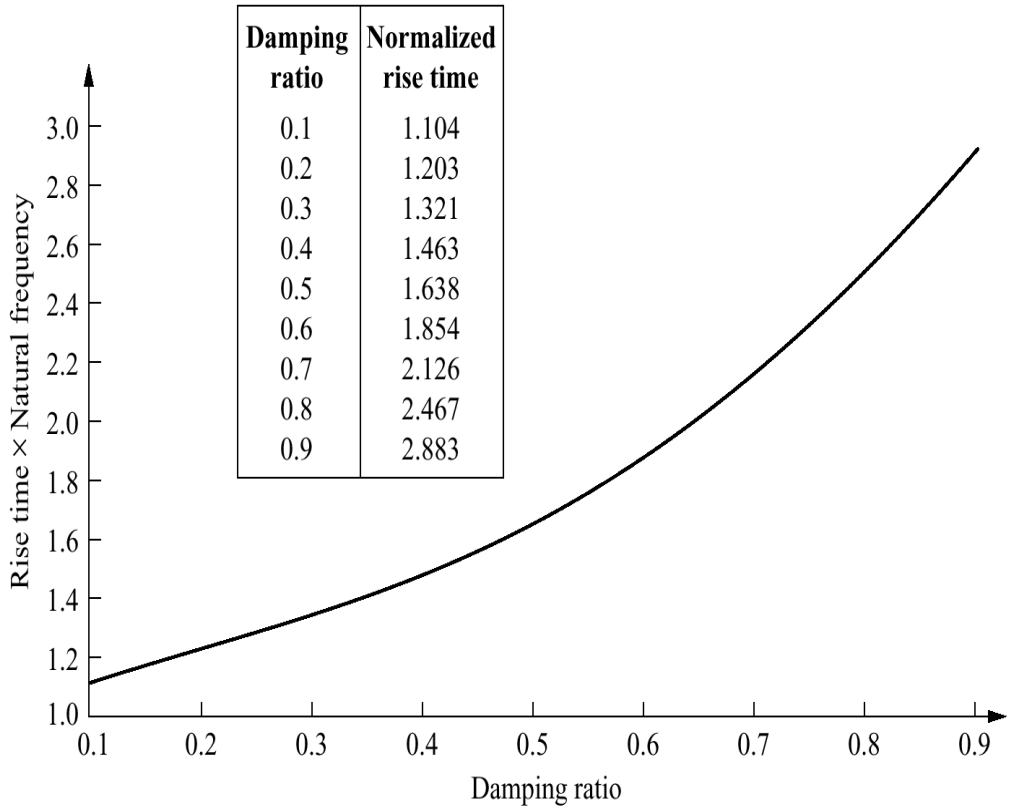

Figure 4.17
Pole plot for an underdamped second-order system

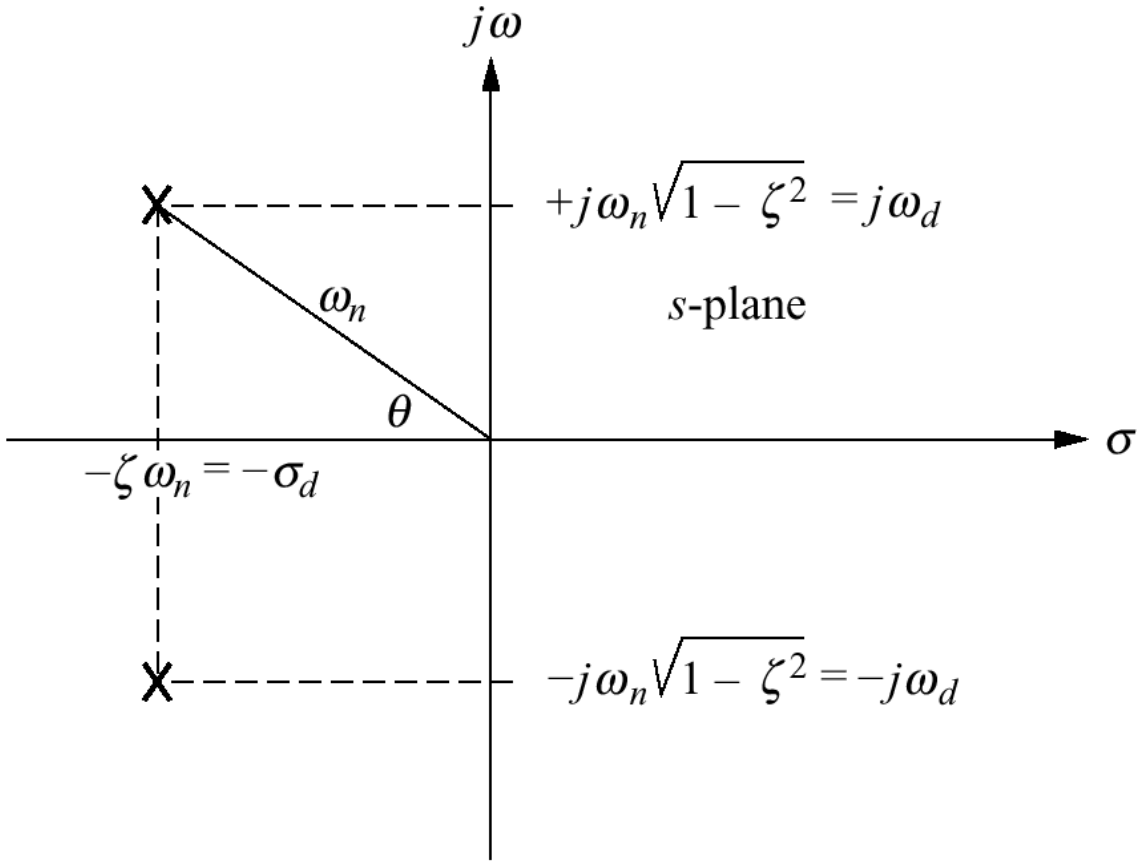

Figure 4.18
Lines of constant peak time, T_p, settling time, T_s, and percent overshoot, %OS
Note: $T_{s_2} < T_{s_1}$; $T_{p_2} < T_{p_1}$; $\%OS_1 < \%OS_2$

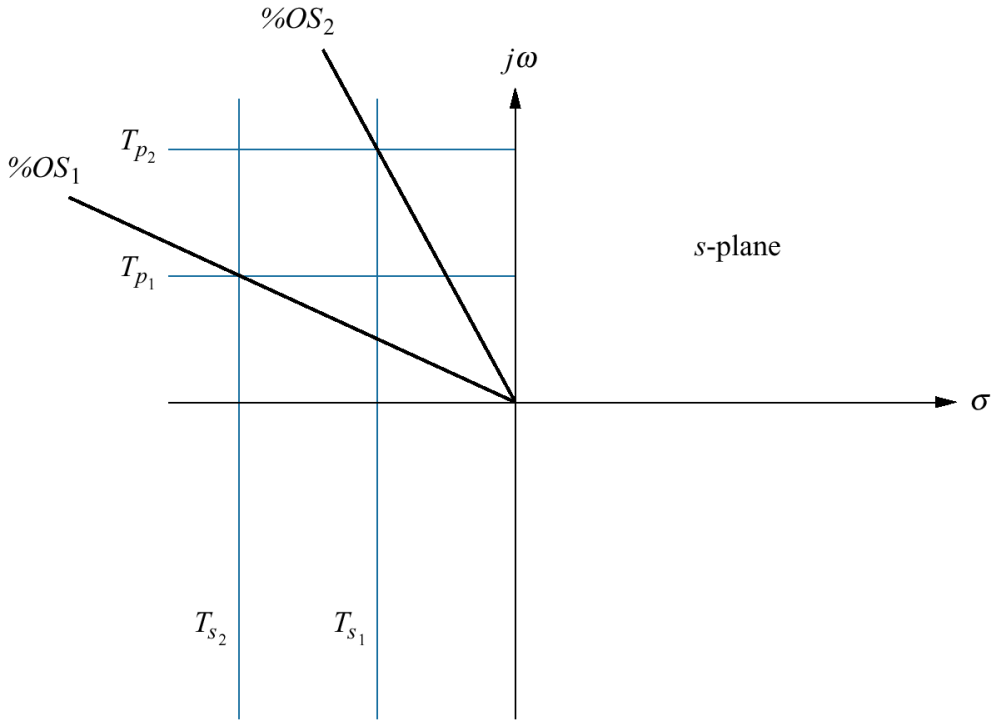

Figure 4.19
Step responses of second-order underdamped systems as poles move:
a. with constant real part;
b. with constant imaginary part;
c. with constant damping ratio

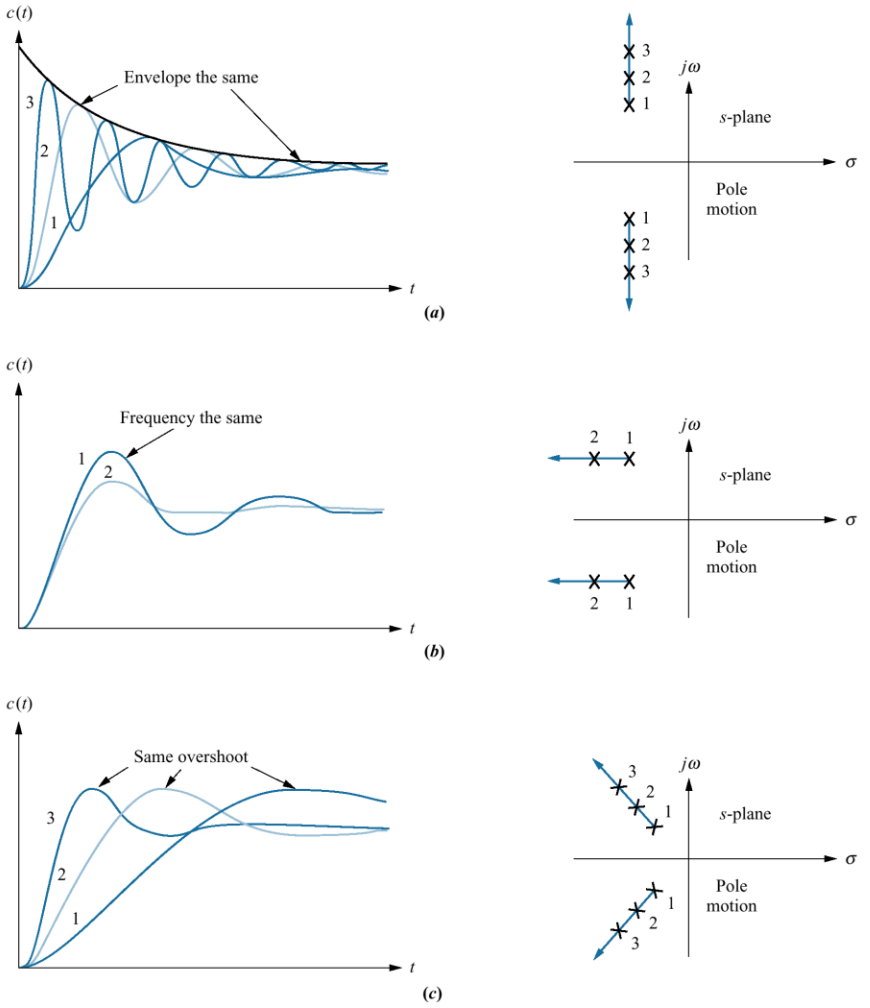

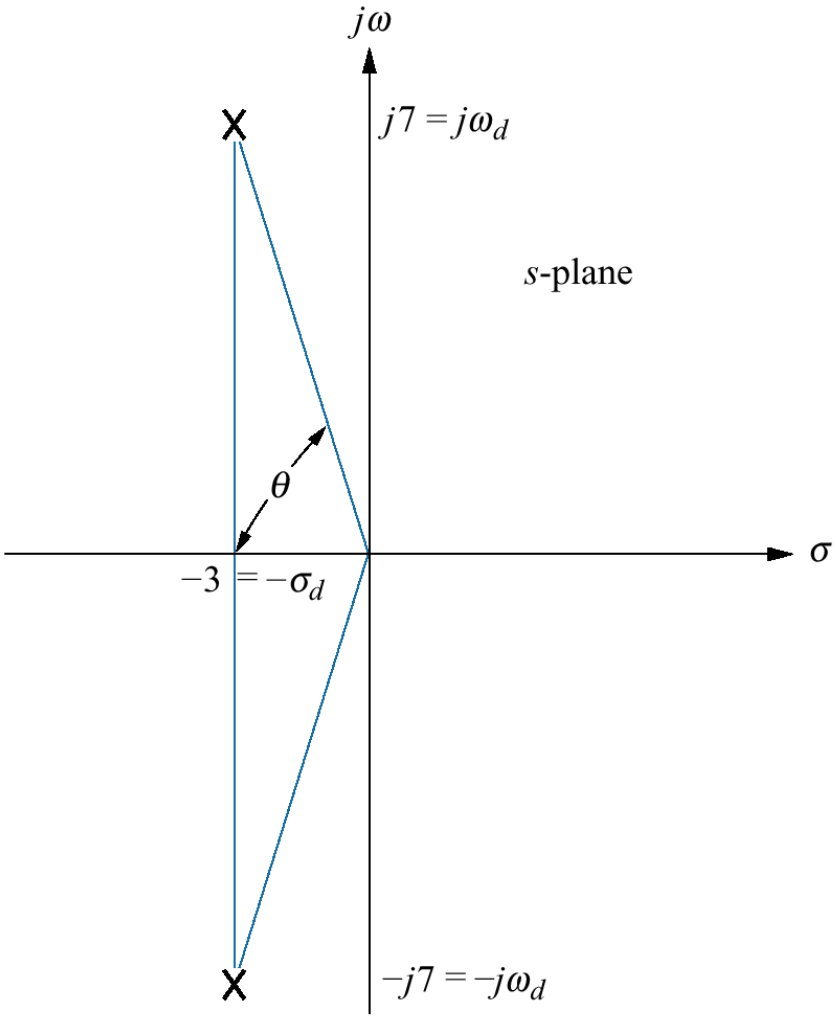

Figure 4.20
Pole plot for
Example 4.6

Figure 4.21
Rotational mechanical system for Example 4.7

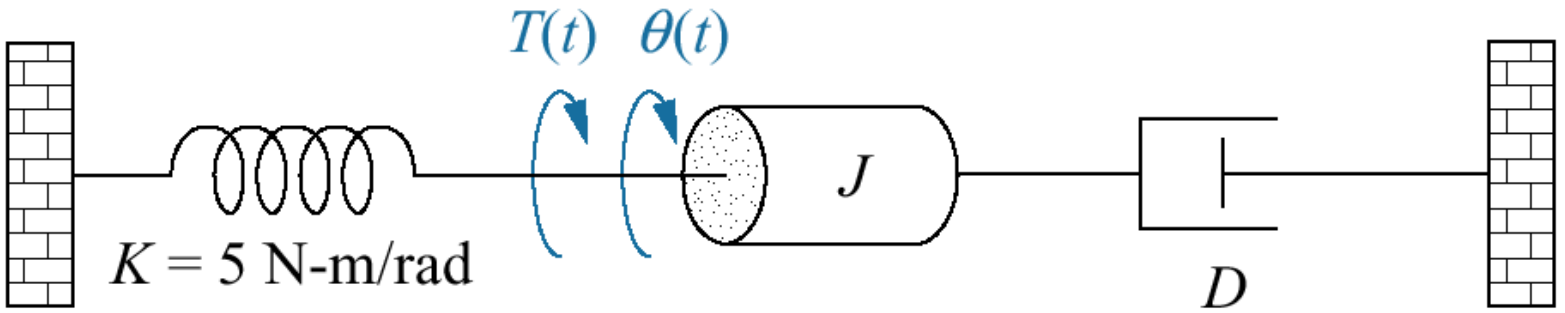

Figure 4.22

The Cybermotion SR3 security robot on patrol. The robot navigates by ultrasound and path programs transmitted from a computer, eliminating the need for guide strips on the floor. It has video capabilities as well as temperature, humidity, fire, intrusion, and gas sensors.

Courtesy of Cybermotion, Inc.

Figure 4.23

Component responses of a three-pole system:
a. pole plot;
b. component responses: nondominant pole is near dominant second-order pair (Case I), far from the pair (Case II), and at infinity (Case III)

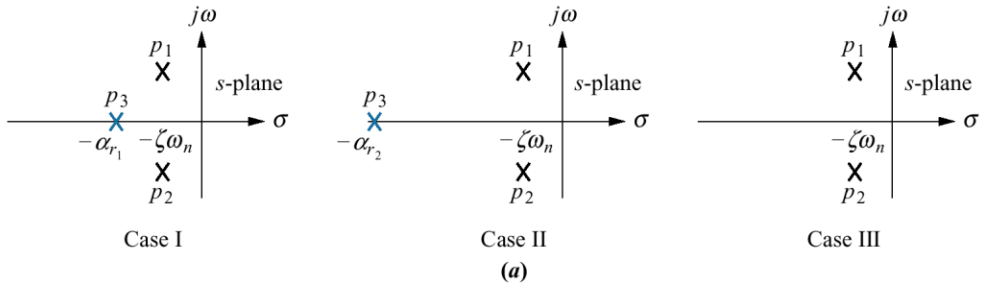

(a)

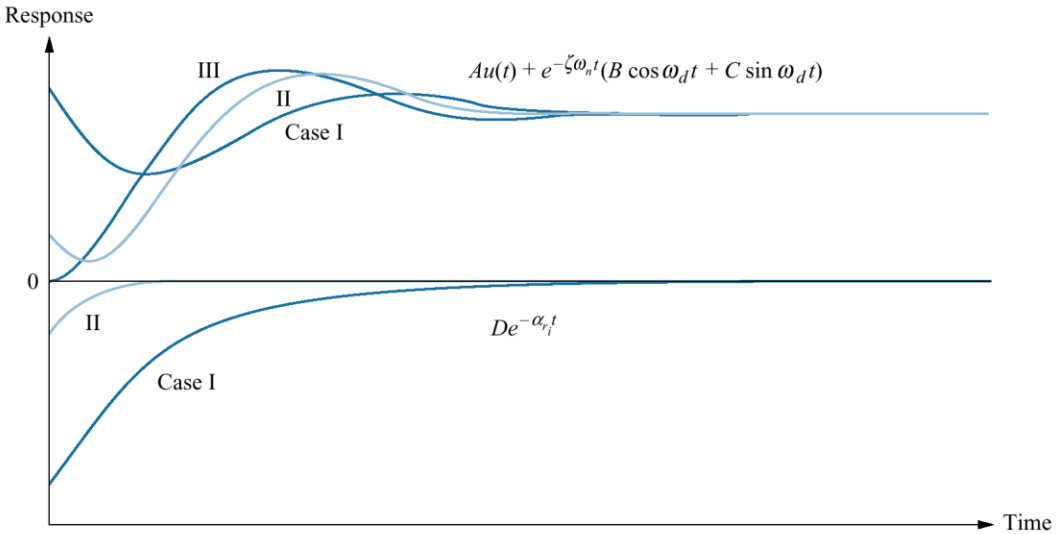

(b)

Figure 4.24
Step responses of system $T_1(s)$, system $T_2(s)$, and system $T_3(s)$

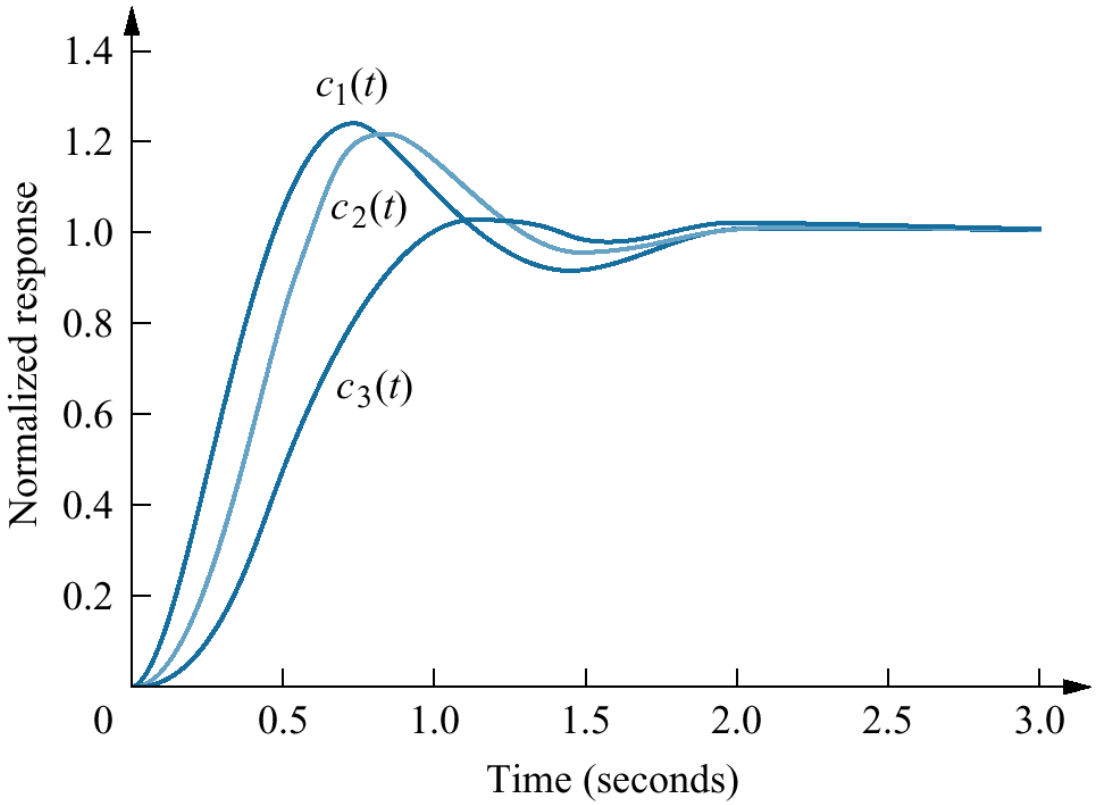

Figure 4.25
Effect of adding a zero to a two-pole system

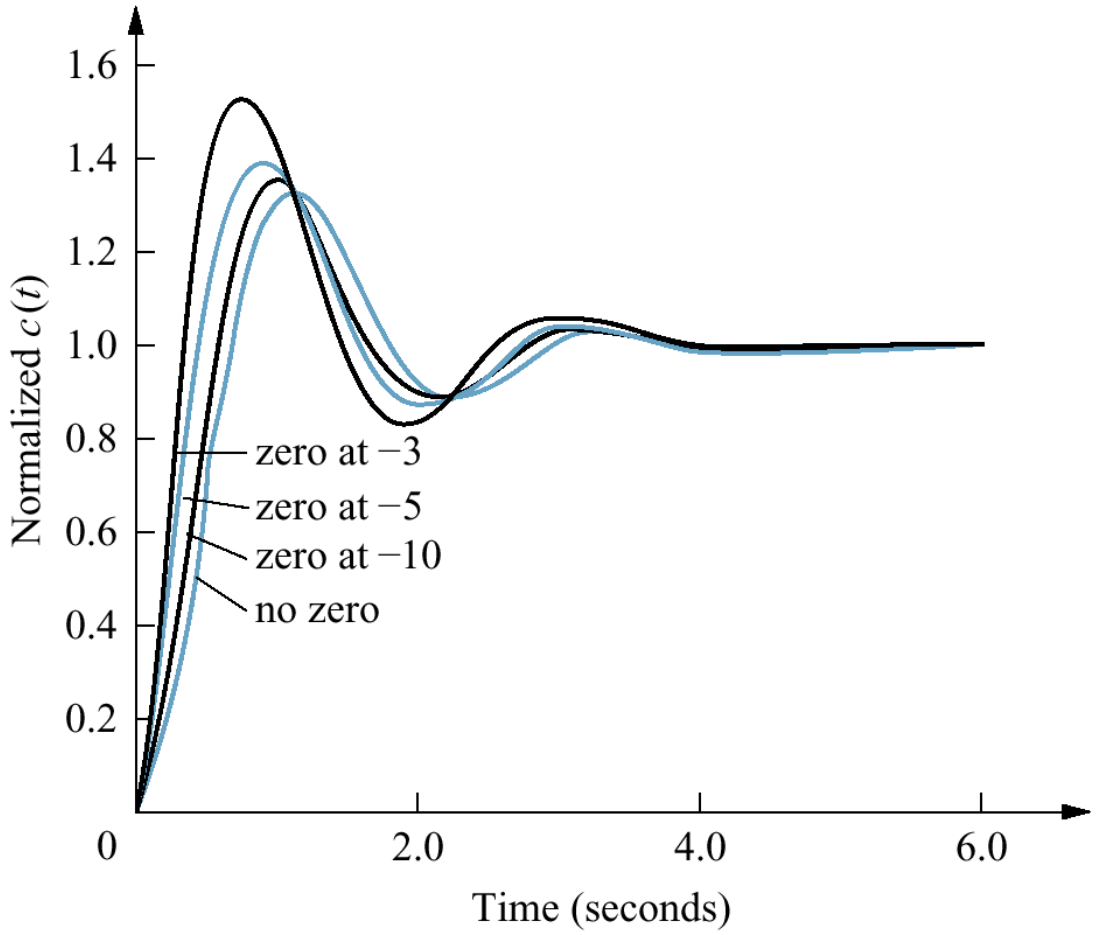

Figure 4.26
Step response of a nonminimum-phase system

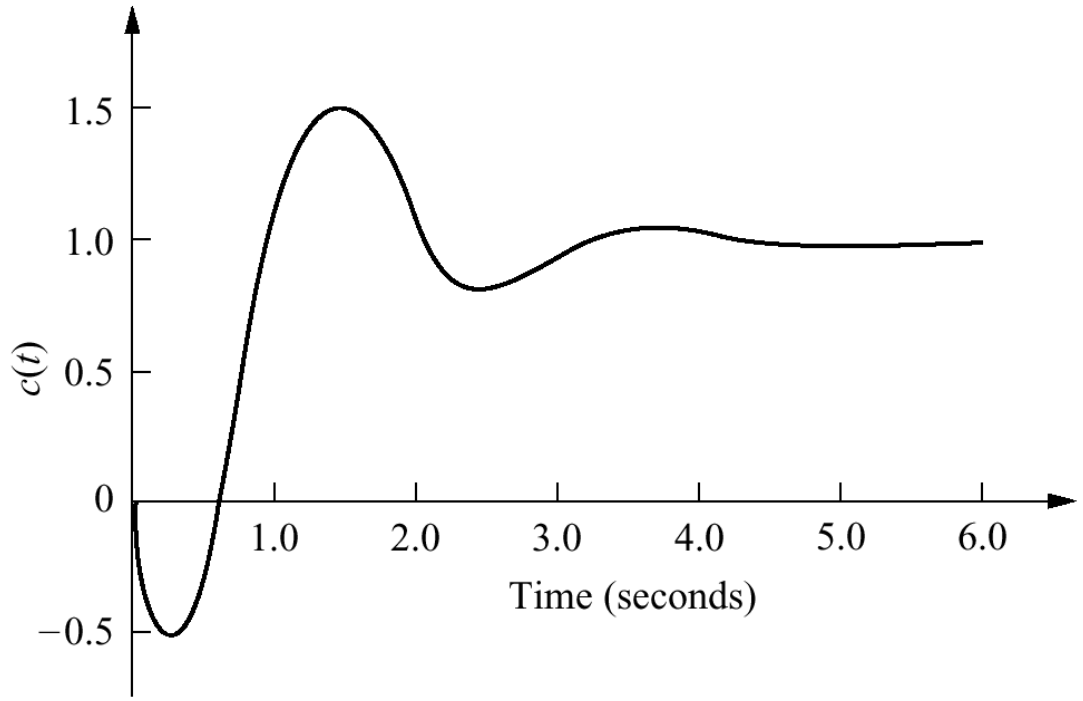

Figure 4.27
Nonminimum-phase electrical circuit

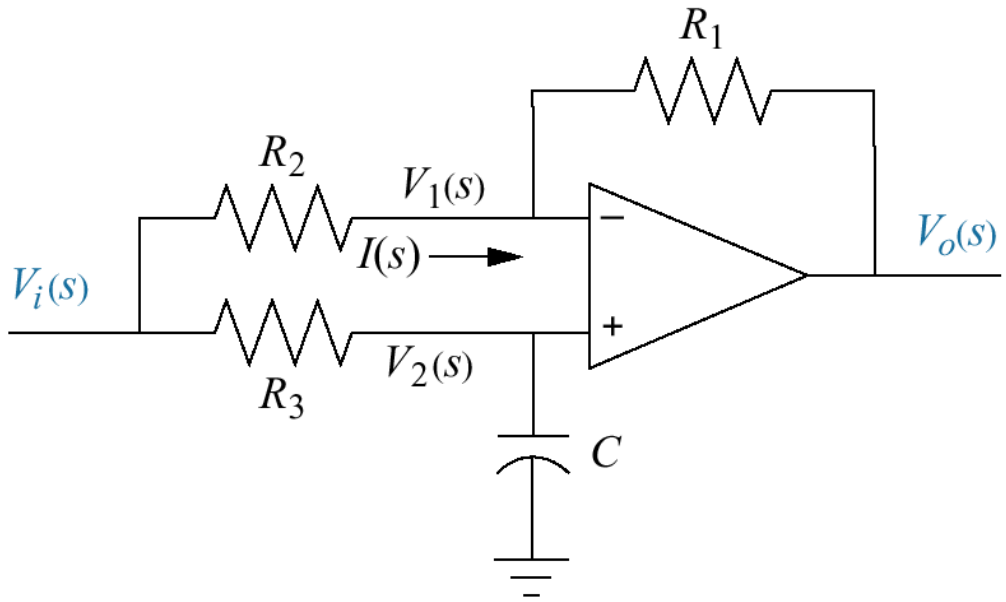

Figure 4.28
Step response of the nonminimum-phase network of Figure 4.27 (c(t)) and normalized step response of an equivalent network without the zero ($-10c_o(t)$)

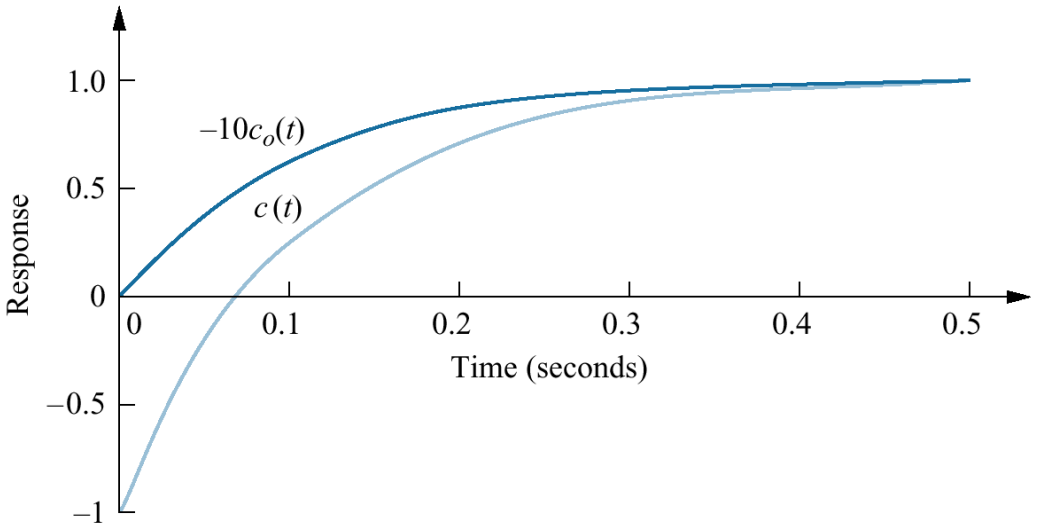

Figure 4.29
a. Effect of amplifier saturation on load angular velocity response;
b. Simulink block diagram

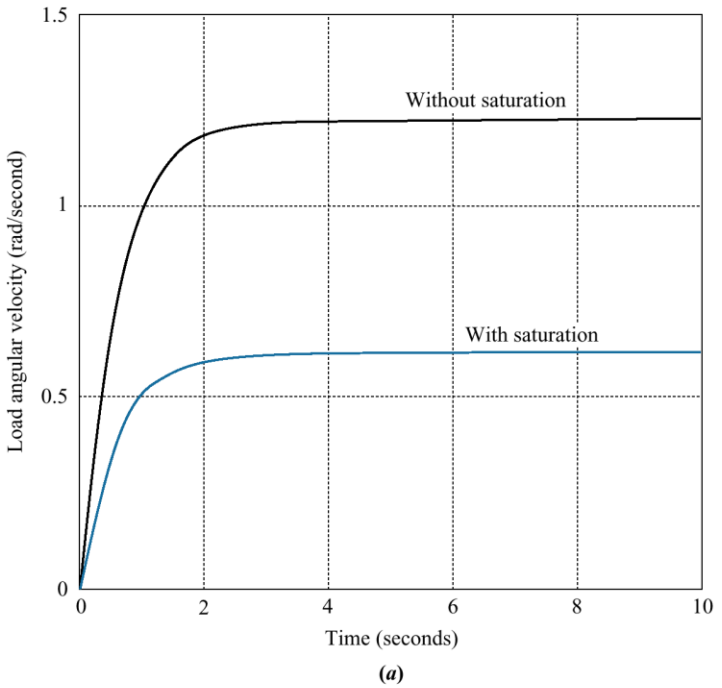

Figure 4.30
a. Effect of deadzone on load angular displacement response;
b. Simulink block diagram

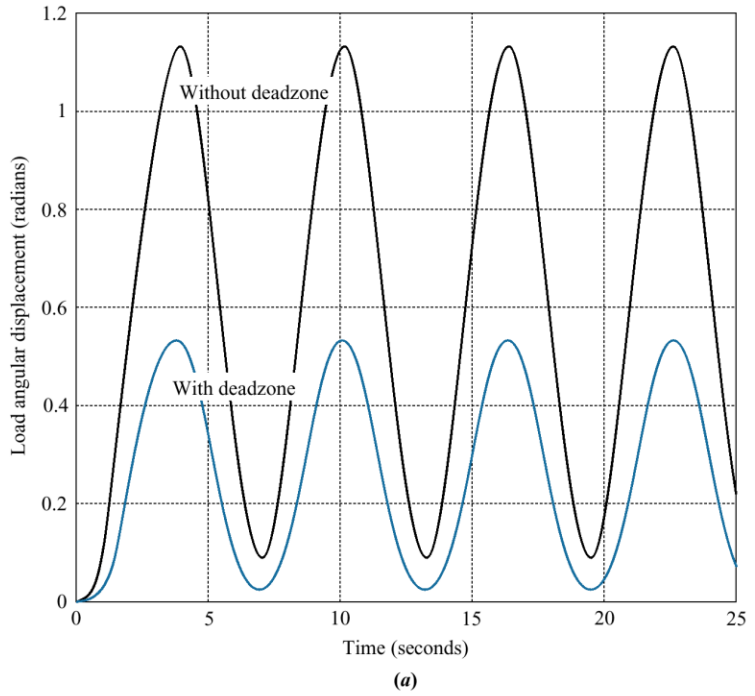

Figure 4.31
a. Effect of backlash on load angular displacement response;
b. Simulink block diagram

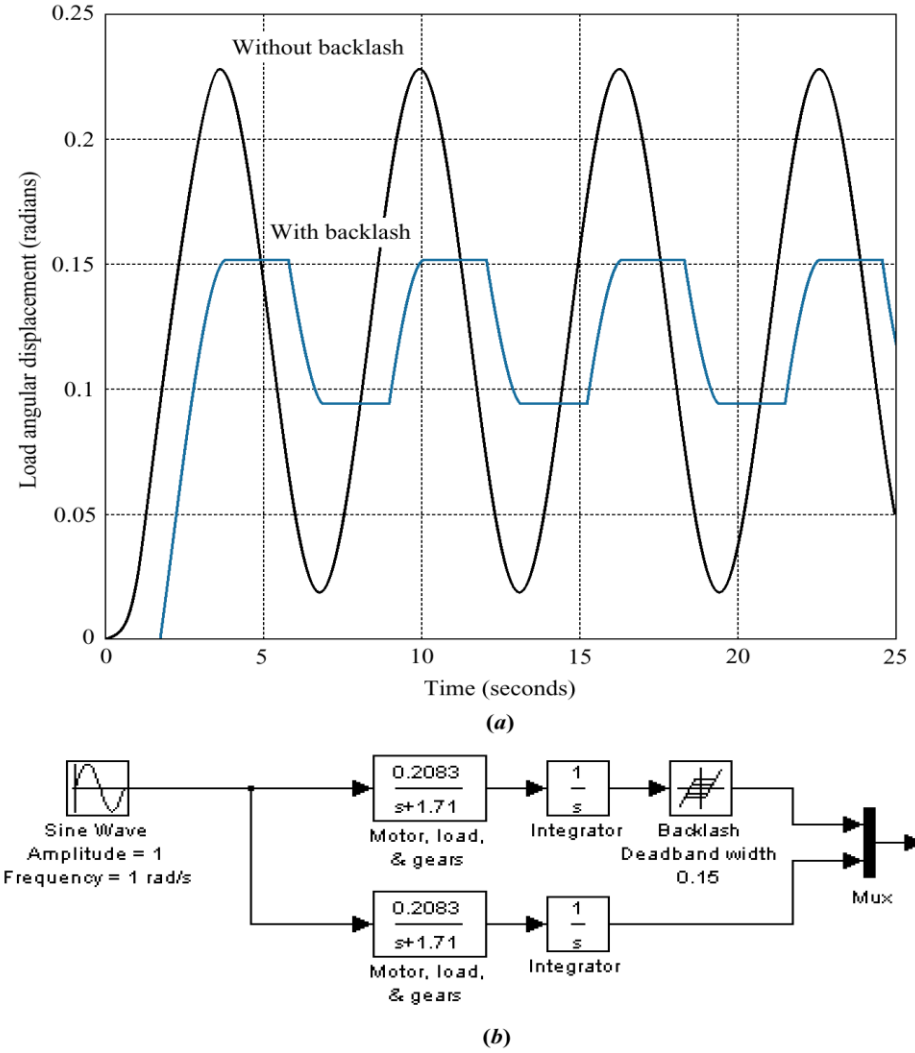

Figure 4.32
Antenna azimuth position control system for angular velocity:
a. forward path;
b. equivalent forward path

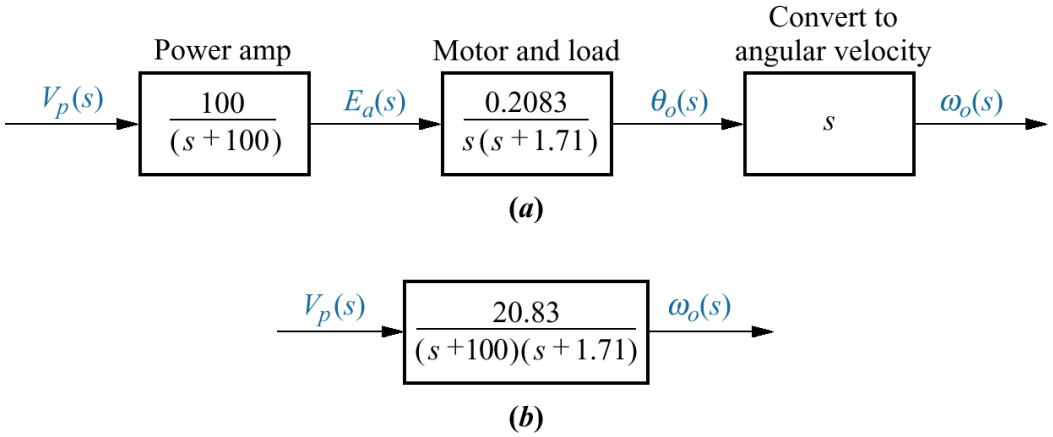

Figure 4.33
Unmanned Free-Swimming Submersible (UFSS) vehicle

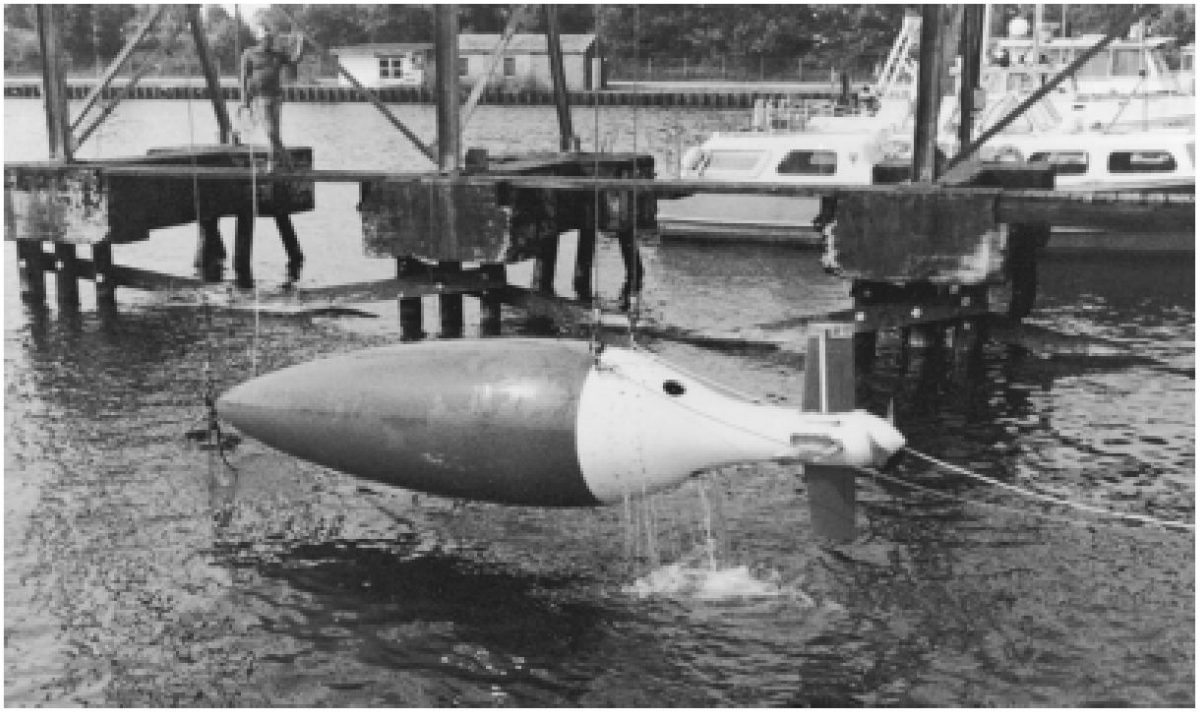

Courtesy of Naval Research Laboratory.

Figure 4.34
Pitch control loop for the UFSS vehicle

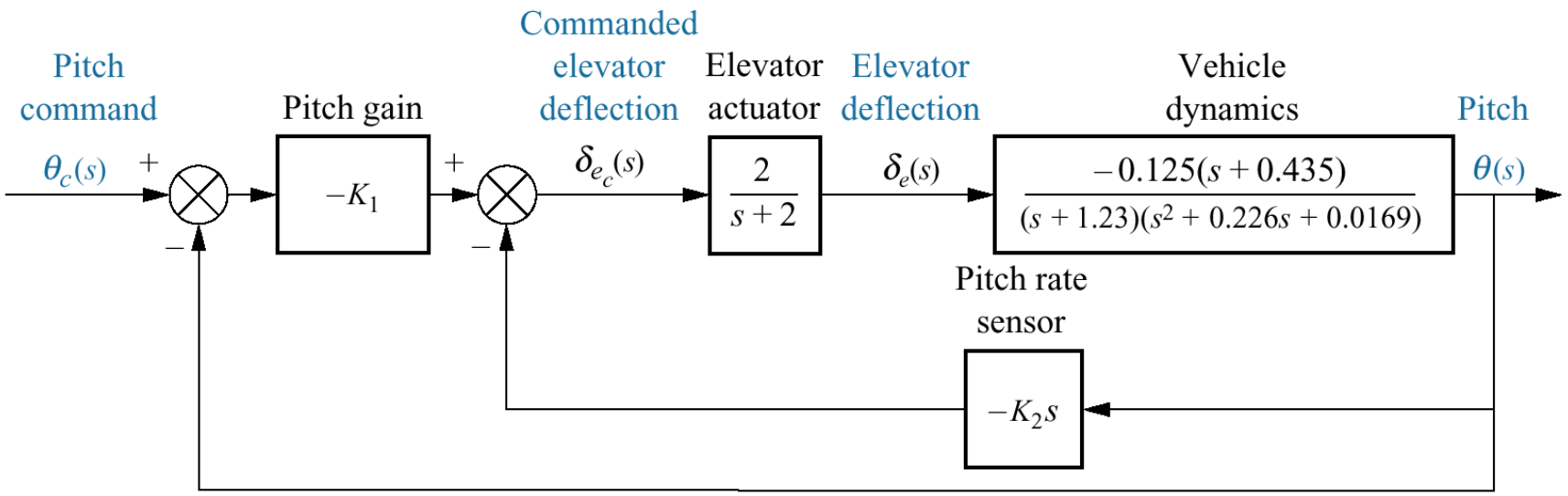

Figure 4.35
Negative step response of pitch control for UFSS vehicle

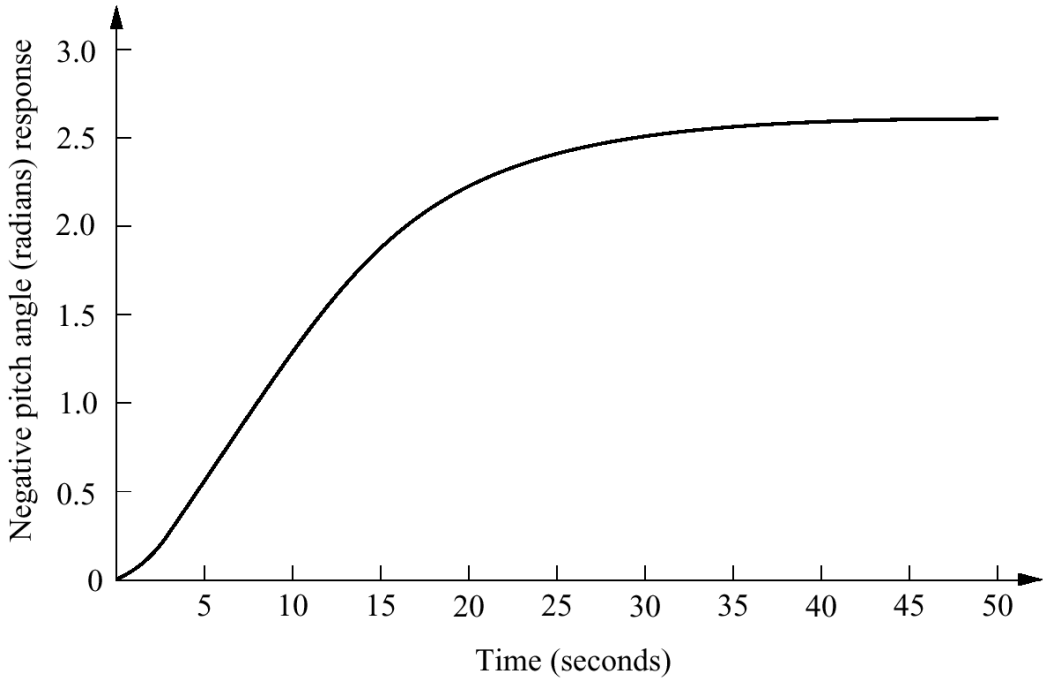

Figure 4.36
A ship at sea, showing roll axis

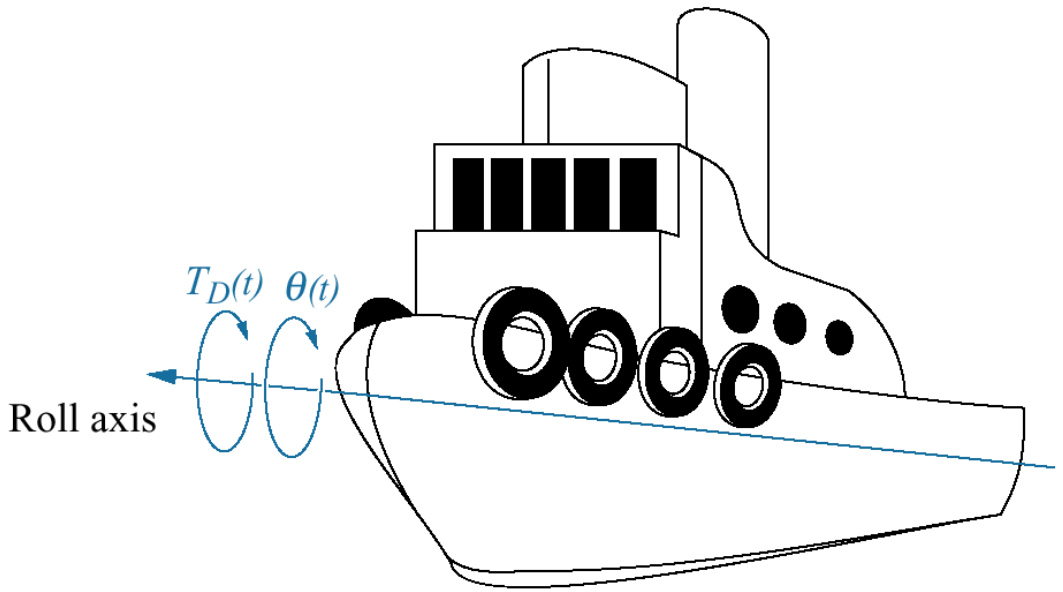

Figure P4.1

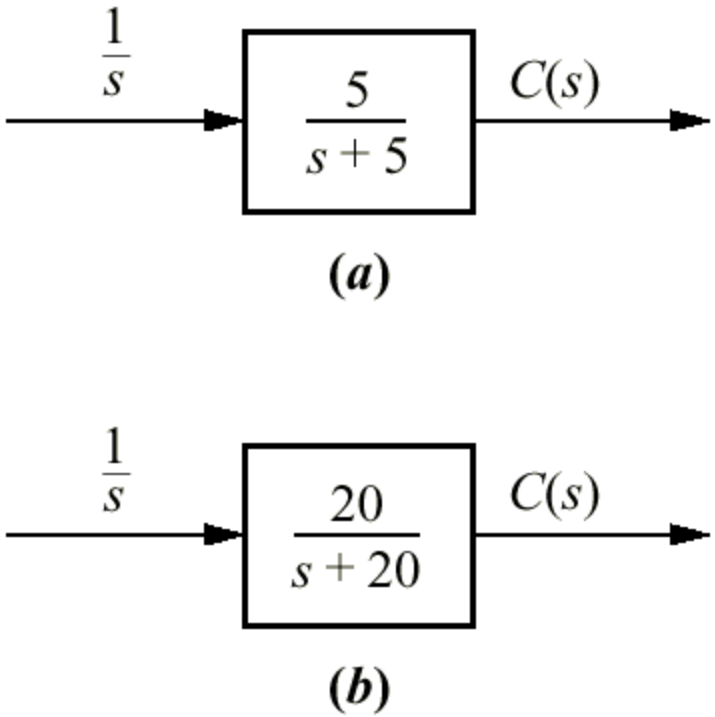

Figure P4.2

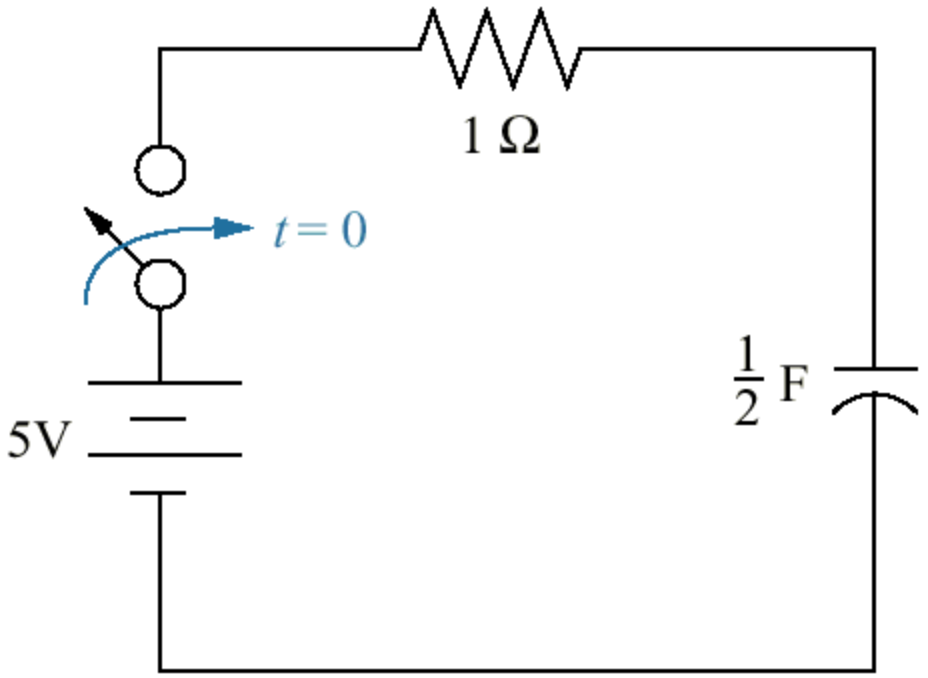

Figure P4.3

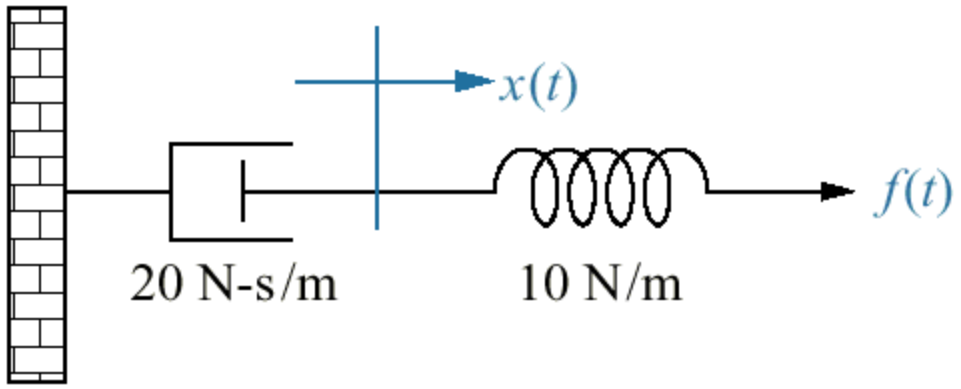

Figure P4.4

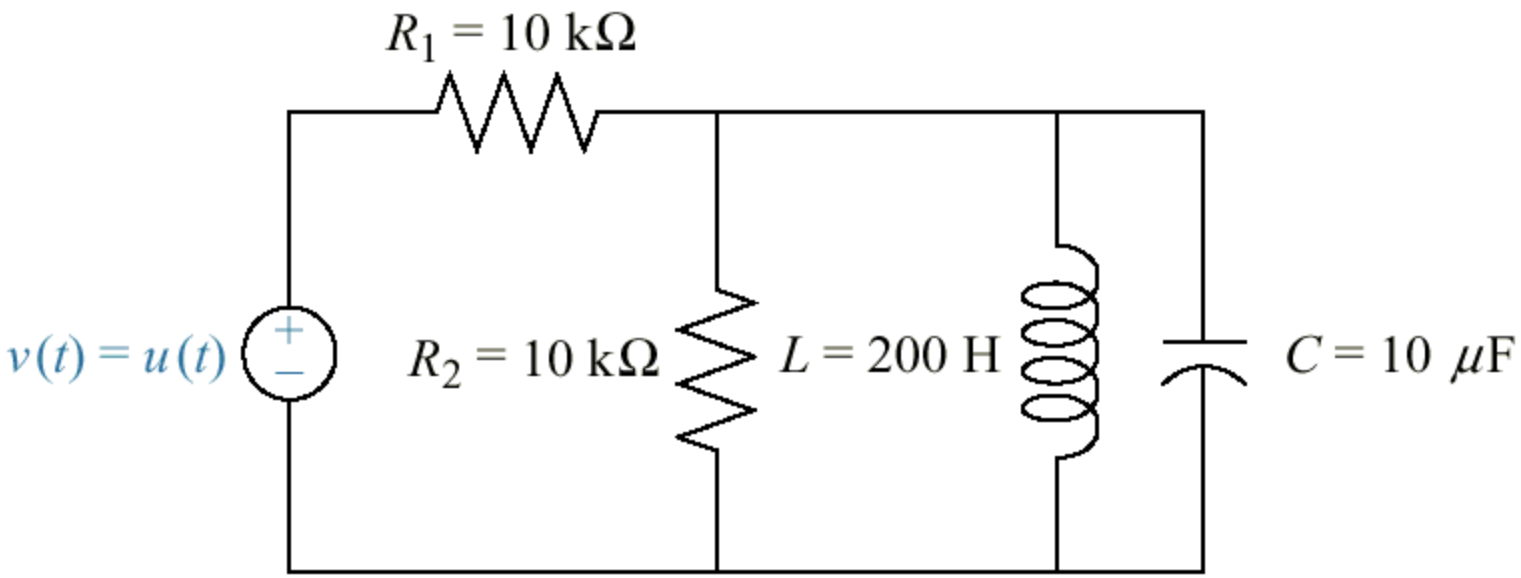
$R_1 = 10\ \text{k}\Omega$
$v(t) = u(t)$
+
−
$R_2 = 10\ \text{k}\Omega$
$L = 200\ \text{H}$
$C = 10\ \mu\text{F}$

Figure P4.5

$M = 1$ kg
$K_s = 5$ N/m
$f_v = 1$ N-s/m
$f(t) = u(t)$ N

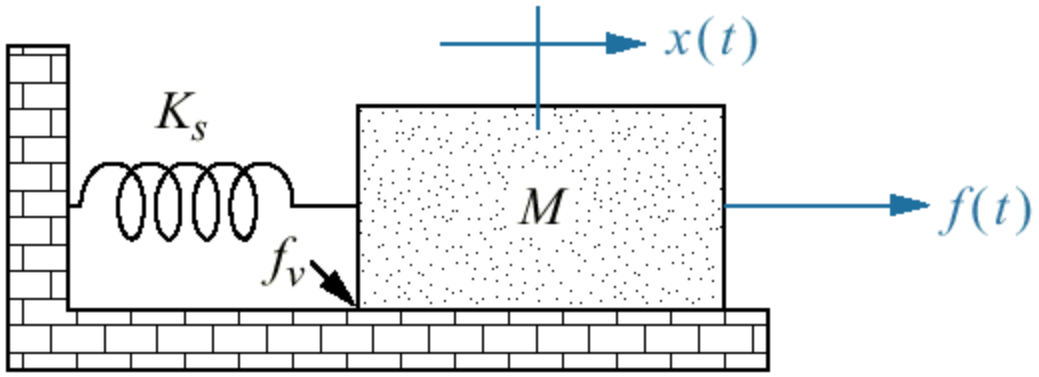

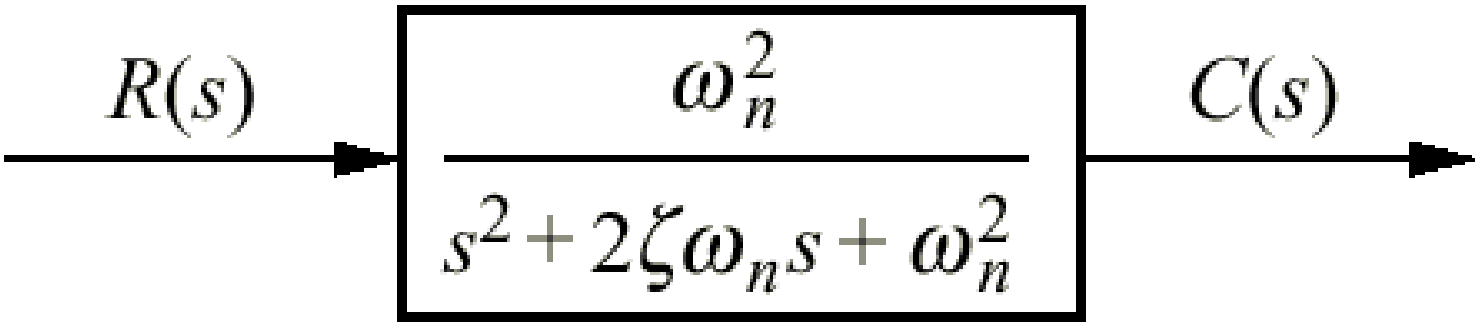

Figure P4.6

Figure P4.7

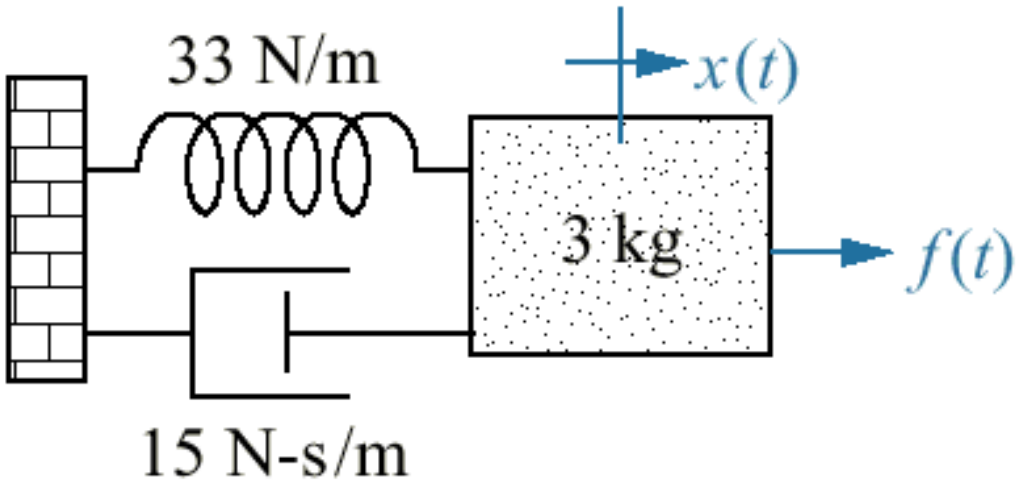

Figure P4.8

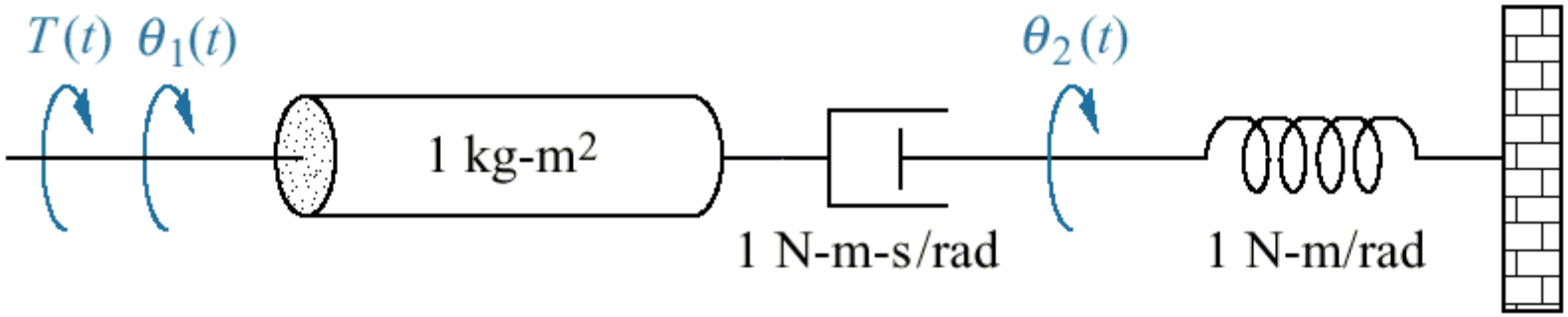

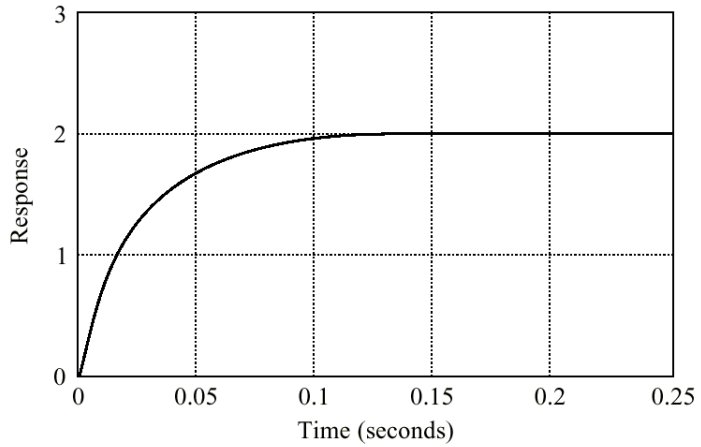

(*a*)

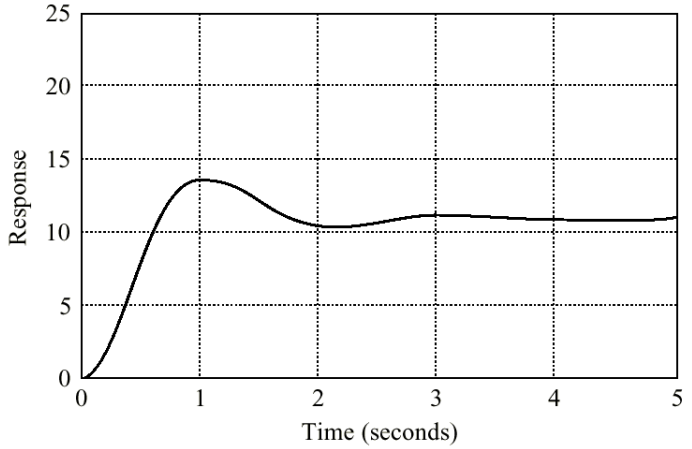

(*b*)

Figure P4.9
(*figure continues*)

Figure P4.9
(*continued*)

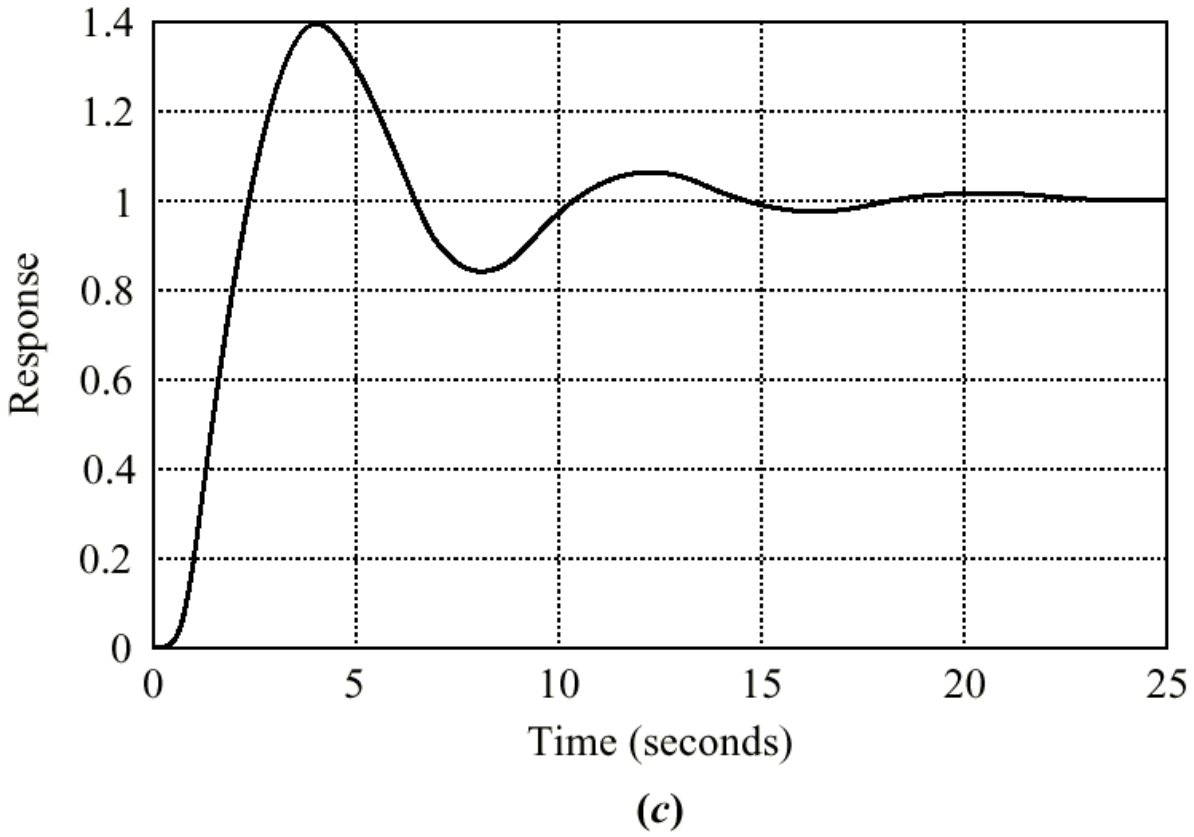

(*c*)

Figure P4.10

Steps in determining the transfer function relating output physical response to the input visual command

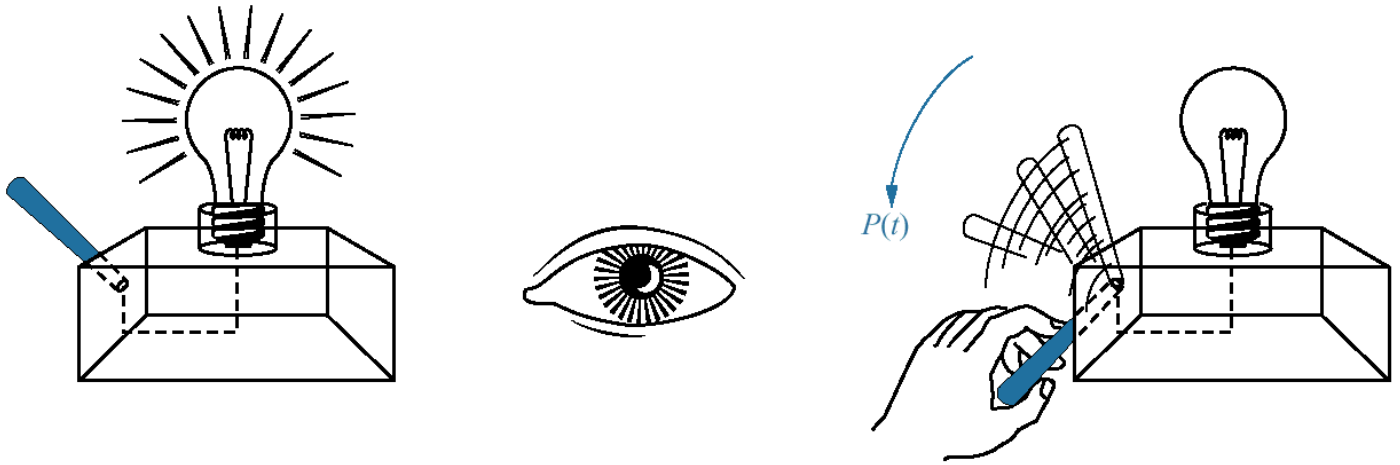

Step 1: Light source on Step 2: Recognize light source Step 3: Respond to light source

Figure P4.11
Vacuum robot
lifts
two bags of salt

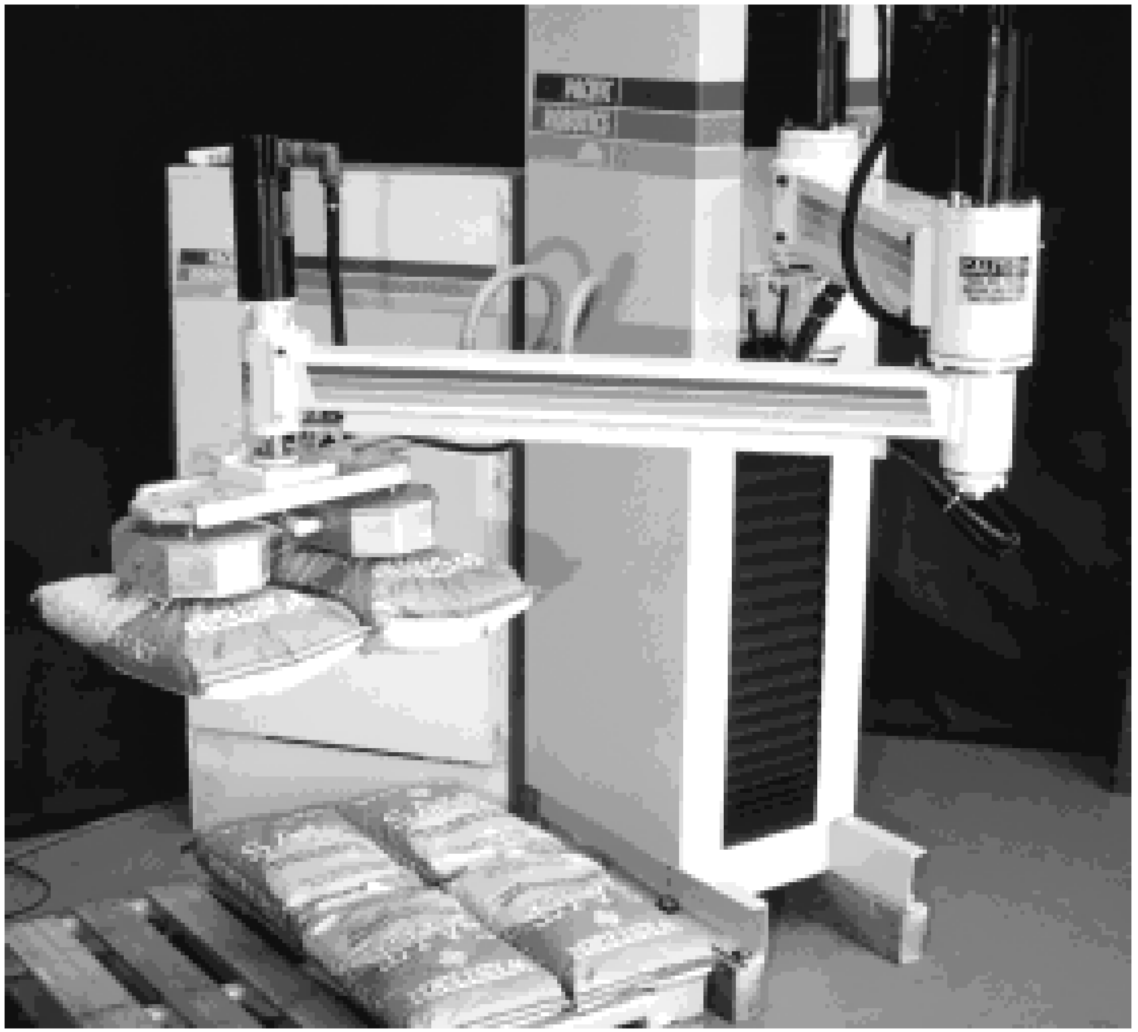

Courtesy of Pacific Robotics, Inc.

Figure P4.12

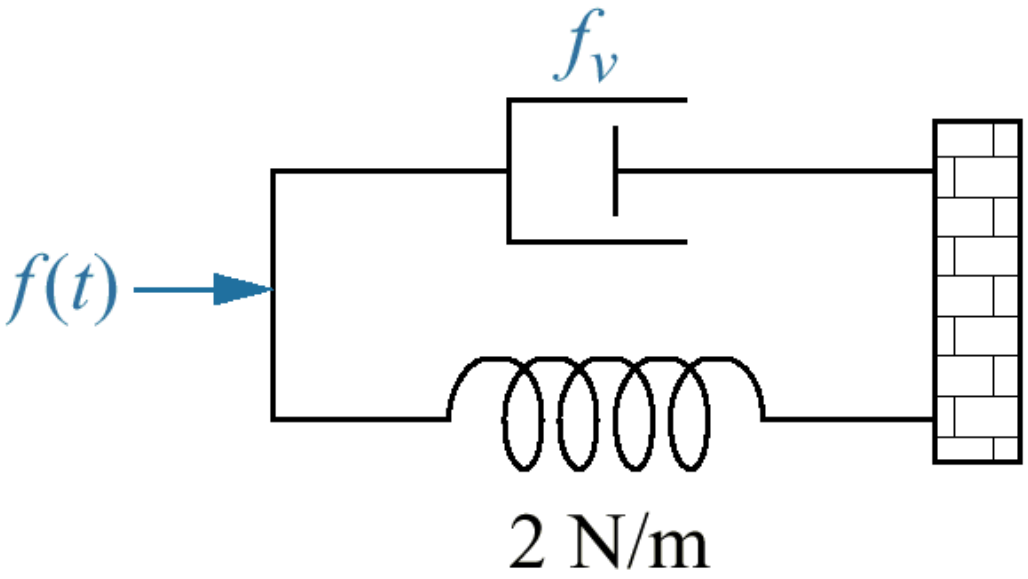

Figure P4.13

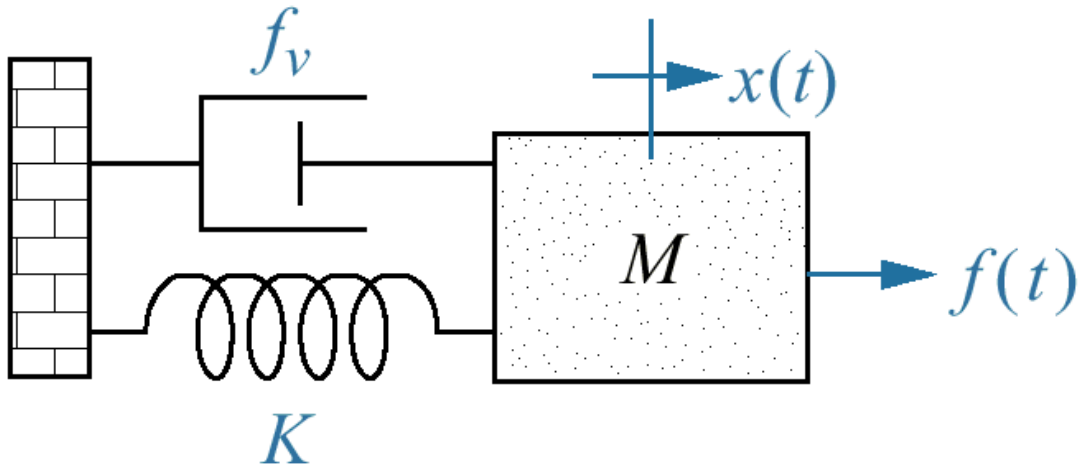

Figure P4.14

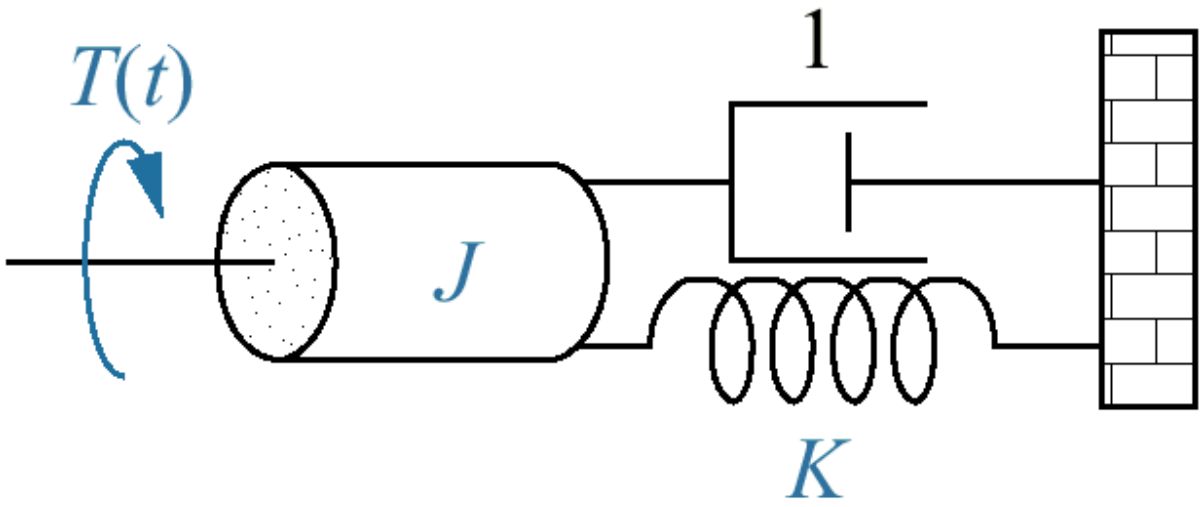

Figure P4.15

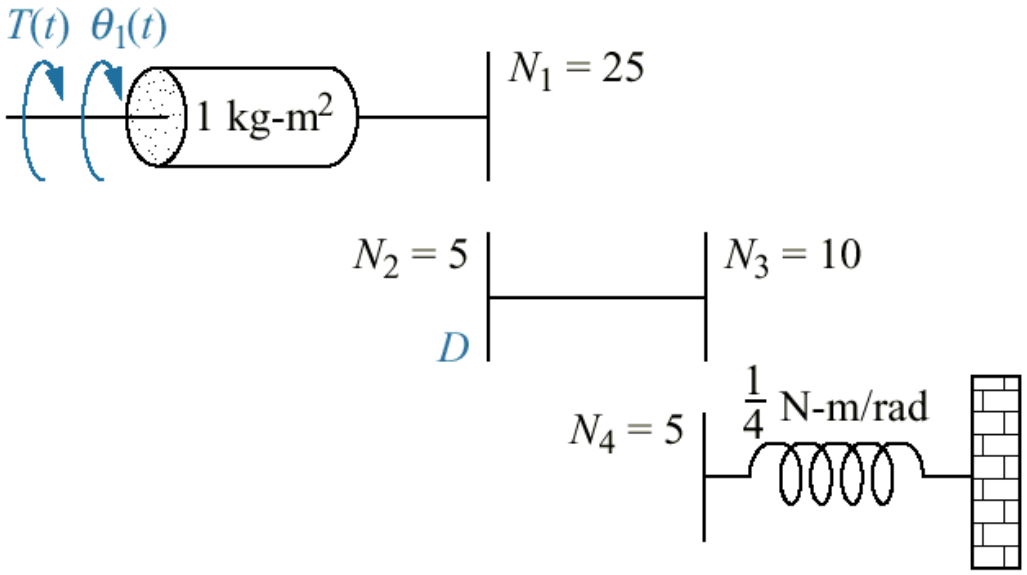

Figure P4.16

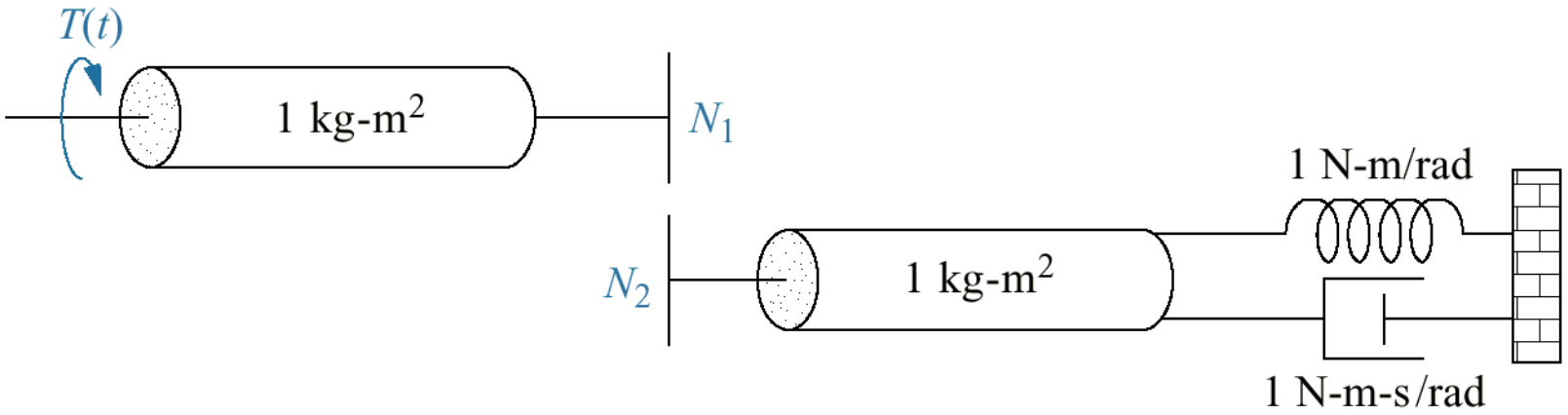

Figure P4.17

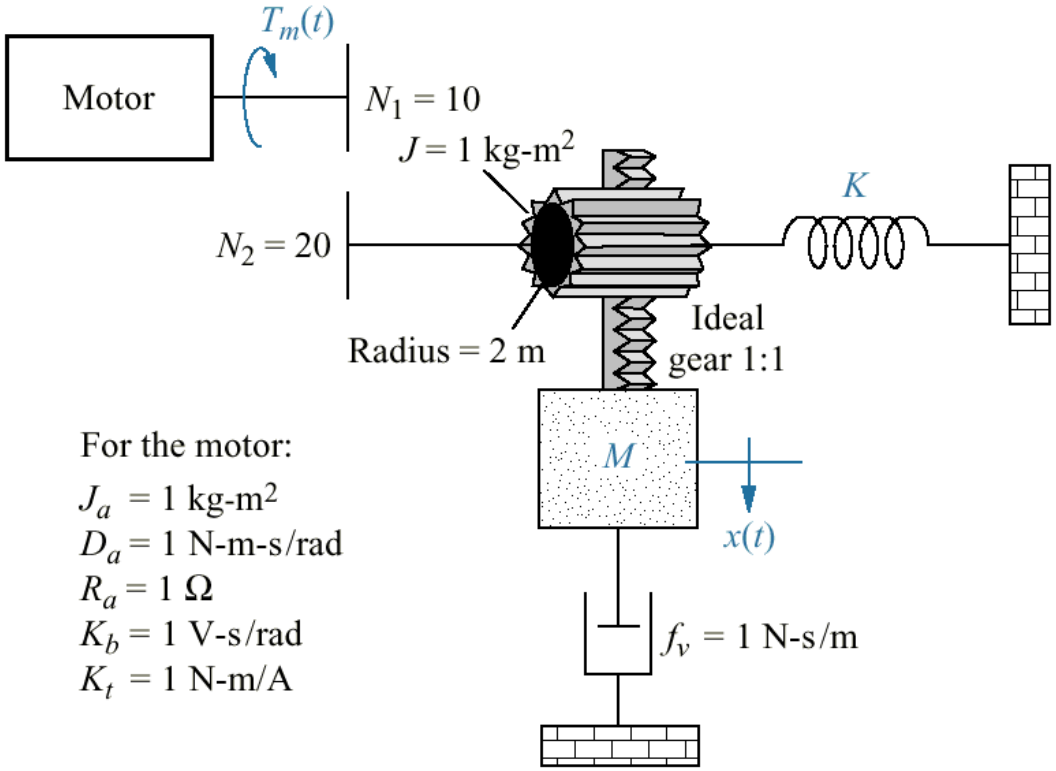
$T_m(t)$
Motor
$N_1 = 10$
$J = 1$ kg-m^2
K
$N_2 = 20$
Ideal
gear 1:1
Radius = 2 m
M
$x(t)$
$f_v = 1$ N-s/m
For the motor:
$J_a = 1$ kg-m^2
$D_a = 1$ N-m-s/rad
$R_a = 1\ \Omega$
$K_b = 1$ V-s/rad
$K_t = 1$ N-m/A

Figure P4.18

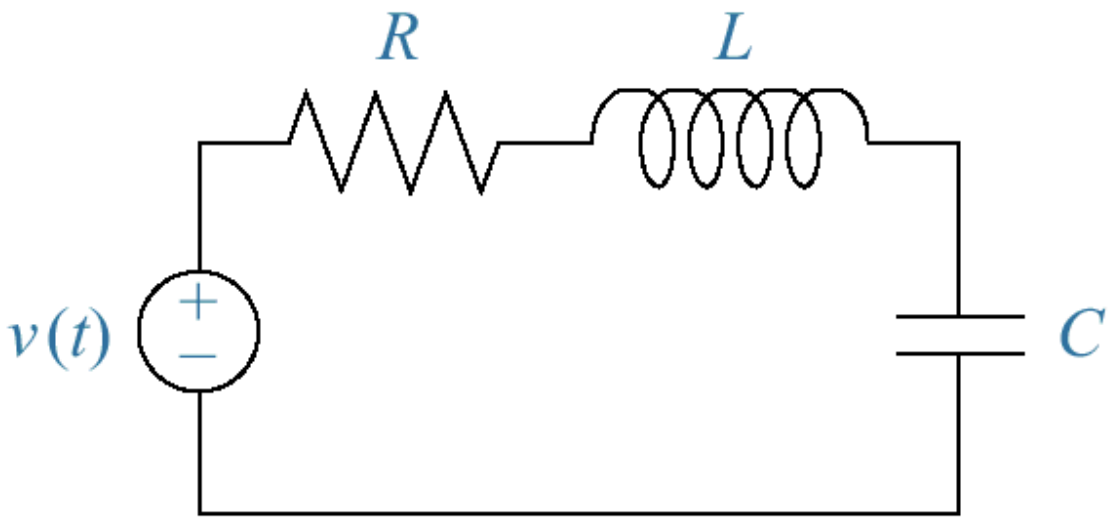

Figure P4.19

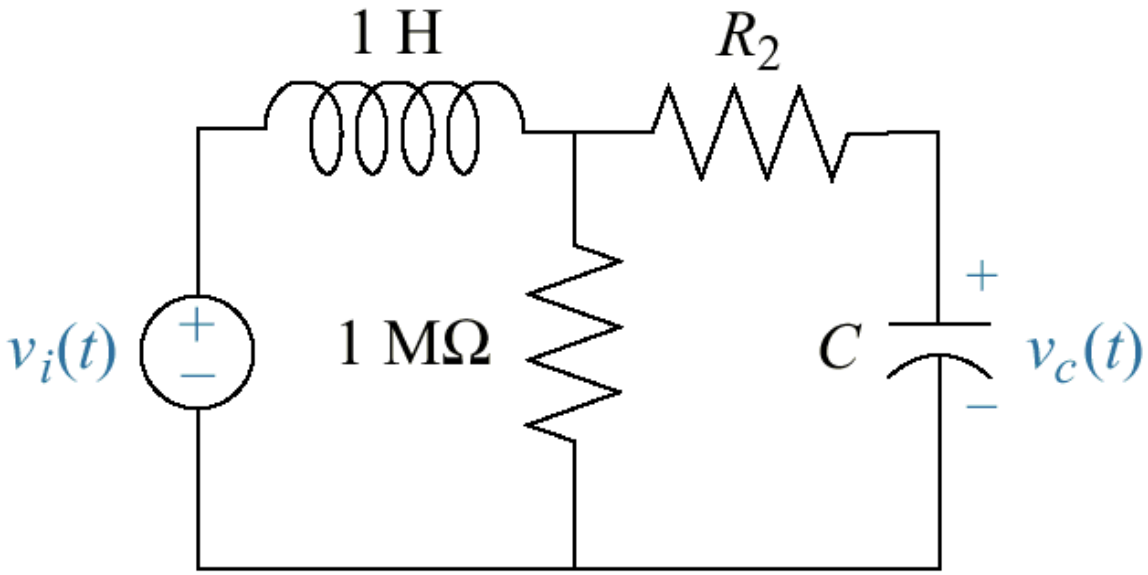

Figure P4.20
Pump diagram